

EMISSIVE ORGANIC RADICALS SUBSTITUTED BY PHOSPHORUS-
CONTAINING MOIETIES: APPLICATIONS AS OLED MATERIALS

by

Ragene Thornton, B.S.

A thesis submitted to the Graduate Council of
Texas State University in partial fulfillment
of the requirements for the degree of
Master of Science
with a Major in Chemistry
August 2019

Committee Members:

Todd Hudnall, Chair

William Brittain, Co-Chair

Benjamin Martin, Co-Chair

COPYRIGHT

by

Ragene Thornton

2019

FAIR USE AND AUTHOR'S PERMISSION STATEMENT

Fair Use

This work is protected by the Copyright Laws of the United States (Public Law 94-553, section 107). Consistent with fair use as defined in the Copyright Laws, brief quotations from this material are allowed with proper acknowledgement. Use of this material for financial gain without the author's express written permission is not allowed.

Duplication Permission

As the copyright holder of this work I, Ragene Thornton, authorize duplication of this work, in whole or in part, for educational or scholarly purposes only.

ACKNOWLEDGEMENTS

To begin, I would like to thank Dr. Hudnall for giving me the opportunity to pursue my passion in his research lab. I would also like to extend this thanks to all the wonderful people in the Hudnall group; I would not have been able to make it through without the care and support from my peers. I have been part of the Hudnall group for two years and throughout my time in the group I have gained friends, wisdom and a family.

I would also like to extend a thanks to the Chemistry/Biochemistry faculty and staff.

A special thank you to my parents and siblings, for loving and supporting me throughout my academic career.

TABLE OF CONTENTS

	Page
ACKNOWLEDGEMENTS	iv
LIST OF FIGURES.....	vii
ABSTRACT.....	ix
CHAPTER	
1. INTRODUCTION	1
1.1 Organic Electronics and the History of OLEDs.....	1
1.2 Organic Emissive Layer	5
1.2.1 Open-Shell Emitters	7
1.3 Pnictogen Heteroles.....	10
2. RESEARCH MOTIVATIONS.....	14
2.1 Research Motivations	14
2.2 Objectives	14
2.3 Spectroscopic and Analytical Tools Used for Characterization	15
3. DIBENZOPHOSPHOLE ANALOGS AND REACTIONS	17
3.1 Introduction.....	17
3.2 Synthesizing dibenzophospholes.....	20
3.3 Addition of Dibenzophospholide into the TTM system.....	25
3.4 Experimental	28
4. DIPHENYLPHOSPHINE ANALOGS AND REACTIONS	40
4.1 Introduction.....	40
4.2 Reactions with Diphenylphosphine	40

4.3 Experimental	41
5. CONCLUSION	44
REFERENCES	46

LIST OF FIGURES

Figure	Page
1. The use of thiophene in OPVs	1
2. Furan is used in OFET systems	2
3. A schematic of the electron transport event that takes place in LEDs.....	3
4. Standard OLED system.....	4
5. The expected increase in the OLED display market over the next couple of years.	5
6. The HOMO and LUMO gaps seen in singlet and triplet state open shell syste	7
7. Fluorescence in closed shell systems vs open shell systems.	8
8. Carbazole substituted TTM radical.....	9
9. The PL and EL of the carabzole-TTM moiety.....	10
10. Cyclopentatdienide pyrrole, phosphole, furan and thiophene	11
11. The HOMO diagrams of the pnictogen heteroles	13
12. The dibenzophospholes and diphenylphosphines of interest	15
13. Prominent dibenzophospholes with optoelectronic properties	18
14. Product 1 ¹ H NMR spectra	29
15. Product 1 ³¹ P NMR spectra.....	29
16. Product 2 ¹ H NMR spectra	30
17. Product 2 ³¹ P NMR spectra.....	31
18. Product 3 ¹ H NMR spectra	32

19. Product 3 ^{31}P NMR spectra.....	33
20. Product 4 ^1H NMR spectra.(Product contained excess starting material.)	34
21. Product 4 ^{31}P NMR spectra.....	35
22. HTTM ^1H NMR spectra.....	36
24. Product 6 ^1H NMR spectra.	38
25. Product 8 ^1H NMR spectra	39
27. Product 10 ^1H NMR spectra	42
28. Product 10 ^{31}P NMR spectra.....	43

ABSTRACT

OLEDs are organic light emitting diodes, meaning that the emitted light is produced by organic molecules rather than solid-state materials used in LEDs. Typical OLEDs undergo emission events via closed shell systems. Radicals are considered “open shell” systems due to their lack of paired electrons. The maximum internal quantum efficiency (IQE) of an open system is 100% because the presence of only doublet states removes conflict with competing electronic states. This is significantly more efficient than the expected 25% IQE seen from fluorescence events in closed shell systems. The radical of interest in this research is tris (2,4,6-trichlorophenyl) methyl or TTM. The goal of the research at hand is to explore the effects of the introduction of pnictogen heteroles into the TTM radical system. Heteroles display attractive optoelectronic applications in organic electronic devices like OLEDs, organic field-effect transistors, and organo-photovoltaics. Carbazole is a heterole that has been at the forefront of OLED chemistry; expansion of research to the rest of the pnictogen group is significantly rarer. The production and analysis of the various heteroradicals should tell us whether the wavelength of the molecule could be tuned, if the quantum yield be adjusted, and if the stability of these molecules be improved. Due to the prevalence of carbazole in OLED systems, exploration of other pnictogen atoms could prove to be groundbreaking. There was success when the cationic form of TTM was used as the replacement for the TTM radical; although there was success, the goal of the research was not fulfilled because the

product produced did not contain a radical anywhere throughout the molecule.

1. INTRODUCTION

1.1 Organic Electronics and the History of OLEDs

The field of organic electronics has grown over the years, owing its success to the desire to obtain both conductive and light-weight materials to be used in the manufacturing of flexible solar cells and more energy efficient light emitting diodes (LEDs).¹ The three primary areas of organic electronics include organic photovoltaics (OPVs), organic field effect transistors (OFETs), and organic light emitting diodes (OLEDs).²⁻⁶ Organic photovoltaics are defined as solar cells that use organic molecules for light absorption and charge transport to produce electricity from sunlight via the photovoltaic effect.⁷ In Figure 1, the nature inspired precursor is a π -conjugated polymer that is typically found in nature as a dye.^{7,8} Photoexcitation of this molecule proves that the implementation of it into OPVs is not beneficial due the immense loss of energy it undergoes via internal conversion.⁷ Functionalizing the nature inspired precursor with thiophene restricts energy loss due to internal conversion and it decreased the bandwidth of the molecule, which in turn increases the absorption rate and promotes easier electron transport.⁷

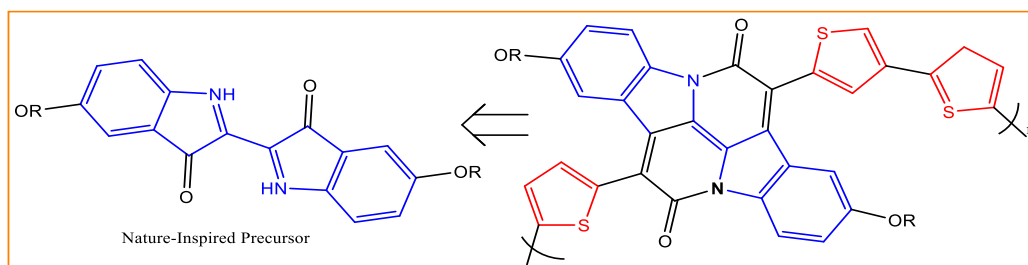


Figure 1. The use of thiophene in OPVs. Thiophene is used to copolymerize with the host materials to decrease the width of the band gap.

Field effect transistors are the building blocks of various display and integrated

circuit systems; the OFET is the organic counterpart. OFETs are composed of a transistor and an induced electric field to manipulate the electrical behavior of the device.^{9, 10} These systems typically contain polymers or thiophene based molecules due to their semi-conducting abilities. In Figure 2, the exploration of furan-based systems rather than thiophene-based showed that furan is just as beneficial as thiophene in OFET systems due to oxygen's smaller Van der Waals radius.^{11, 12} Discoveries like these have contributed to increased interest in organo-electronics.

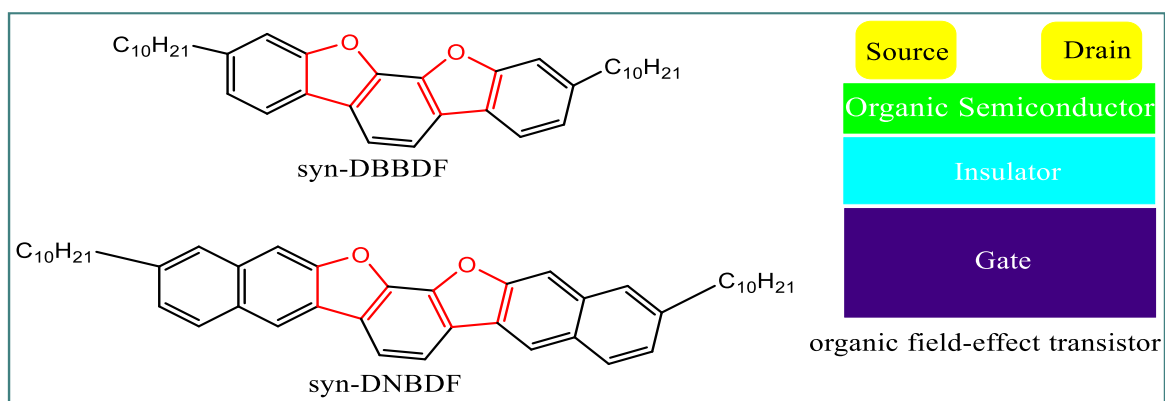


Figure 2. Furan is used in OFET systems due to their semiconducting abilities and dense packing structure.

OLEDs are organic light emitting diodes, where the emitted light is produced by organic molecules rather than solid-state inorganic materials used in traditional LEDs. OLEDs are the organic and subsequently inexpensive and light weight counterpart of LEDs. Moreover, OLEDs can be lighter and more flexible, and they offer the potential for improvements in picture quality when compared to conventional LEDs.^{13, 14} A LED, seen in Figure 3, is defined as a junction diode with a forward bias.¹ A diode contains a forward bias only if the anodic electrode sustains a positive charge and the cathodic electrode sustains a negative charge. The forward bias in a LED is created by opposing junctions. The n-type (or cathodic) junction produces electrons and the p-type (or anodic)

junction produces positive points that lack electrons, which are referred to as “holes”. As current is produced in the system the electrons and holes travel to opposite electrodes. When the electrons and holes recombine in the junction, they release energy in the form of photons of light.

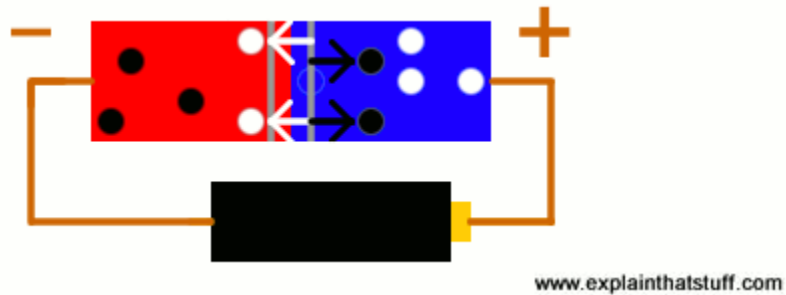


Figure 3. A schematic of the electron transport event that takes place in LEDs ¹⁵.)

In an OLED (Figure 4) the n and p type junctions are comprised of organic materials. When a voltage is applied to the electrodes in an OLED, a similar electroluminescence event occurs; however, the current flows from the cathode to the anode through multiple layers of organic materials into the emissive layer. The holes are produced at the anode/p-type junction and electrons are produced at the cathode/n-type junction. When the holes and the electrons meet in the emissive layer, they release a burst of energy called a photon.

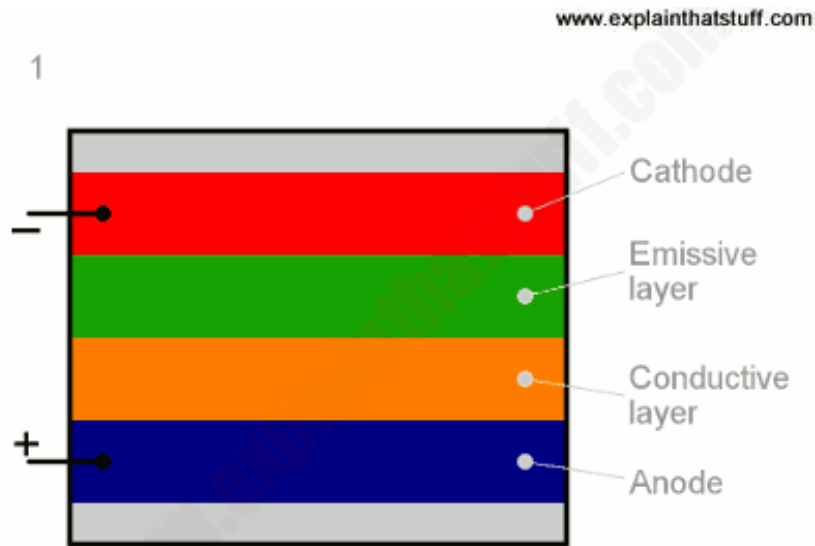


Figure 4. Standard OLED system. ¹⁵

OLEDs have a rich history. Despite their discovery in the mid-20th century, the ultimate performance of OLEDs has yet to be achieved.¹⁶ Emissive organic materials were first discovered in 1953 by the Bernanose group.¹⁶ The group witnessed light emission after doping a cellulose film with the dyeing agent acridine orange. The next milestone was achieved in 1963; the Pope group reported light emission from a crystal of anthracene after they induced carrier injection within a high electric field.^{17, 18} Although there were other minor discoveries during this time, the research developed did not reveal much about the potential of the light emitting organic materials. This misunderstanding was mainly due to issues with low efficiency and luminescence in conjunction with the need for high electric fields.¹⁹ The next breakthrough was made by Tang and VanSlyke of Eastman Kodak in 1987.¹⁹ The duo reported particularly bright emission from a device with a structure different from earlier OLEDs.²⁰ The Tang-VanSlyke device contained a pair of thin organic layers housed between two electrodes.²⁰ The two-layer structure consisted of separate hole transporting and electron transporting layers such that

recombination and light emission occurred in the middle of the organic layer.²⁰ This event resulted in a reduction in operating voltage and improvements in efficiency. Tang and VanSlyke reported light emission from a voltage as low as 2.5V and a power efficiency of 1.51 lm/W; in contrast they also reported an external quantum efficiency (EQE) of only 1%.²⁰ Despite this drawback, the device gained lots of attention, both in industrial and academic research fields. The industry grew immensely throughout the years and in 1997 the world's first commercial OLED was created as the display for a car radio.^{19, 21} A year later, in 1998, phosphorescent OLEDs which utilize triplet emitters were invented.²² These discoveries led to the prevalent use of OLEDs in modern day electronics. OLEDs can be found in a variety of digital devices such as television systems, media players, handheld devices and computer monitors. Figure 5 displays the projected growth of the OLED market from 2016-2026.

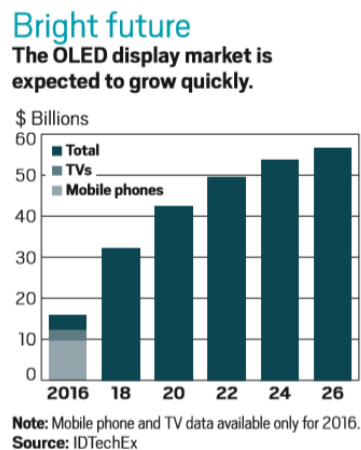


Figure 5. The expected increase in the OLED display market over the next couple of decades.²³

1.2 Organic Emissive Layer

Currently, there are three types of organic materials used in OLEDs: fluorescent, phosphorescent, and thermally activated delayed fluorescent (TADF) materials.²⁴⁻²⁶ The

difference between these types of materials is the mechanism employed to achieve the emission of light. When an electron is excited from the singlet ground state, it can either form a singlet or triplet excited state. The direction of the spin of the excited electron determines whether it is singlet or triplet and transitions of a triplet exciton to the ground state is forbidden due to the Pauli Exclusion Principle.²⁷ The singlet state (following the Pauli Exclusion Principle) corresponds to a state where the electron spins are paired, and a triplet state corresponds a set of spin unpaired/parallel electrons. Fluorescence occurs when the excited electron relaxes is excited to a higher energy level relaxes to a lower energy state, and then falls back to the ground state releasing a photon of light. Even though fluorescent events occur readily; they lack in efficiency, specifically internal quantum efficiency (IQE). IQE is defined as the ratio of the number of photons collected to the number absorbed.^{28, 29} An ideal IQE is as close to 100% as possible; this implies that every photon is absorbed and subsequently collected at the electrodes.²⁹ As mentioned before, a fluorescent event consists of an electron emitting light when returning to a singlet ground state from a singlet excited state. The lowest triplet excited state is very close in energy to the singlet ground state and statistically triplet states outnumber singlet states 3:1. This causes fluorescent emitters to suffer because of the prevalence of triplet states (Figure 6). Radiative decay from triplet state is spin forbidden, so the max IQE of these events is only 25%. In contrast, phosphorescence occurs when an electron in the triplet excited state relaxes radiatively to the ground state with the release of a photon of light. One form of this radiative relaxation is a phenomenon known as intersystem crossing (ISC). Intersystem crossing occurs when singlet or triplet excited states non-radiatively convert to the opposite type of state.³⁰ During this time the spin of

the electron is reversed and the resultant radiative decay from the excited triplet state back down to a singlet ground state to release a photon of light is known as phosphorescence.³¹ This type of radiative decay is spin forbidden, however emission through this pathway is promoted through the use of heavy atoms. The presence of heavy atoms affects the photophysical and photochemical processes in a molecule through relativistic effects and spin-orbit coupling which ultimately allows forbidden spin transitions to occur radiatively.³² Because the heavy atom effect requires the use of rare and expensive metals, such as Ir or Pt,^{33, 34} this method of emission is also viewed as inefficient.

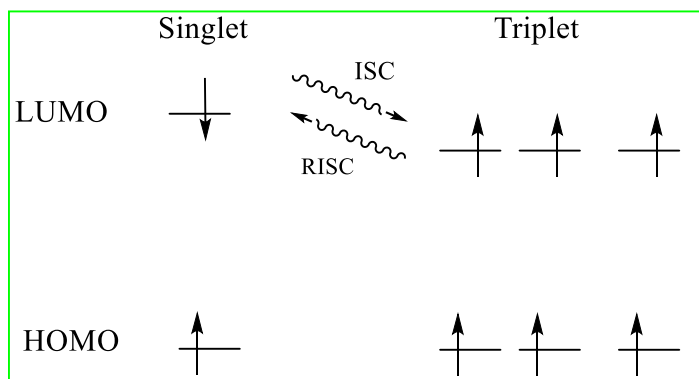


Figure 6. The HOMO and LUMO gaps seen in singlet and triplet state open shell systems

Thermally activated delayed fluorescence (TADF) is another emission technique that is growing in popularity. This technique involves using thermal energy to convert an electron in a triplet excited state to the singlet excited state, where it then emits in a fluorescence event.^{25, 26, 33, 35, 36} This process is termed reverse intersystem crossing (RISC) and it negates any spin forbidden processes.³³

1.2.1 Open-Shell Emitters

Most fluorescence and phosphorescence events are derived from “closed shell”

systems which contain two spin paired or unpaired electrons, respectively. In closed shell systems, there are two electrons in the highest occupied molecular orbital (HOMO).

When the molecule is excited, one electron is promoted to the lowest unoccupied molecular orbital (LUMO), in the excited state while the other electron remains in the HOMO. Radical systems are considered “open shell,” as they contain a single, unpaired electron. Emission from open shell radical systems are like closed shell systems, with the exception that only doublet ground and excited states are possible (an electron is capable of having two spins, hence a “doublet”) rather than singlet and triplet excited state (Figure 7). When a radical is excited, its unpaired electron in its singly occupied molecular orbital (SOMO) is excited to the next singly unoccupied molecular orbital (SUMO). Transitions back to the SOMO are always spin allowed because there is no remaining electron to cause spin parity issues with the excited electron in the SUMO. Therefore, the theoretical maximum IQE of an open shell system is 100% because the presence of only doublet states removes conflict with competing electronic states.^{37, 38} Radical systems are not subject to loss of excitons through non-radiative relaxation because there are no energy states between the doublet ground and excited states.³⁹

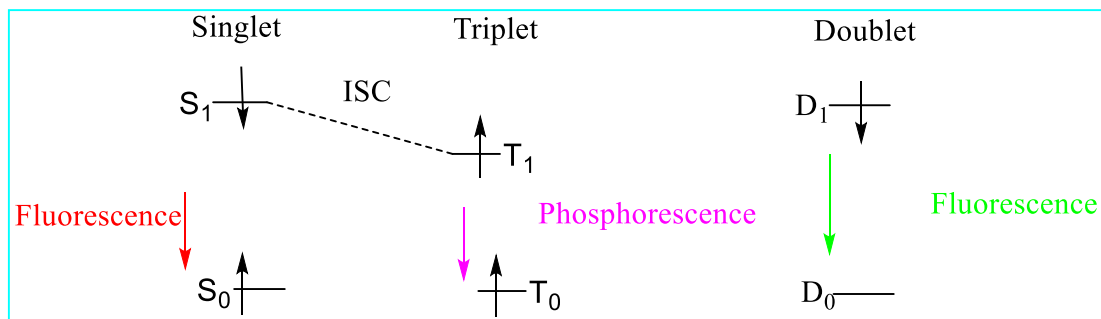


Figure 7. Fluorescence in closed shell systems vs open shell systems.

The use of radicals as doublet emitters in OLEDs has garnered attention recently because the possibility of an IQE of 100%.⁴⁰ This inherent phenomenon, coupled with the expected advancements in the device design of OLEDs, could lead OLEDs to be very competitive in the display market. Doublet emitters also have the ability to produce long emission wavelengths despite the lack of π conjugation.³⁷

This thesis research will focus on derivatizing the known emissive and air stable radical, tris-(2,4,6-trichlorophenyl) methyl or TTM.³⁹ This compound is composed of a methyl radical stabilized by three chlorine substituted benzene rings. These bulky halogenated aryl groups act as protection for the radical causing the radical to be stable under ambient condition however it decomposes after photo-irradiation.⁴¹ To enhance the stability upon photolysis, and to increase the IQE, carbazole or pyridyl units have been installed into TTM radicals (Figure 8). These compounds have been incorporated into OLEDs that exhibit intense red emission and modest IQEs.^{39, 42, 43}

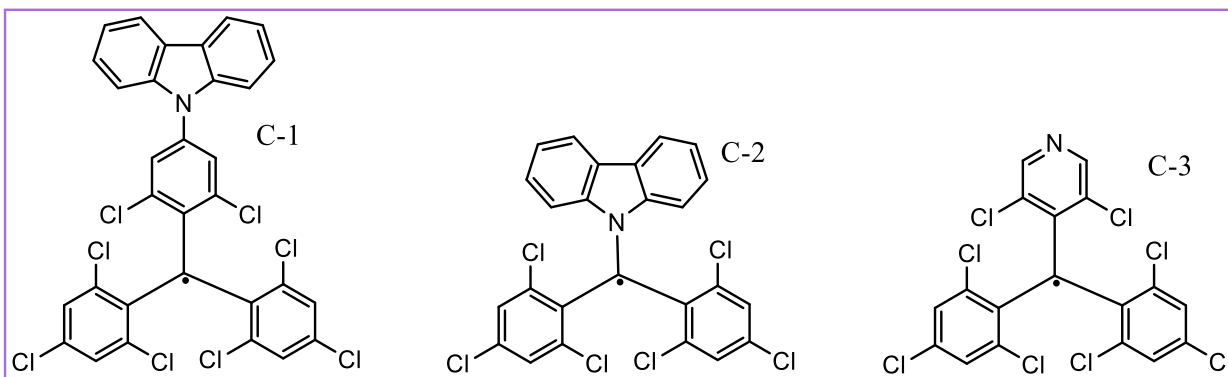


Figure 8. Carbazole substituted TTM radical.

The OLED device constructed from molecule C-1 produced the electroluminescent (EL) and photoluminescent (PL) spectra seen in Figure 9. The device emits in the red region of the visible light spectrum. The Li group was able to confirm

that the emission is due to a transition from the SUMO to SOMO due to the 660nm peak seen in the PL spectra.³⁹ This transition was further confirmed via the absorbance spectra. A band centered at 600nm corresponds to an energy gap of 2.07eV; which is attributed to the transition between the SUMO and SOMO.³⁹

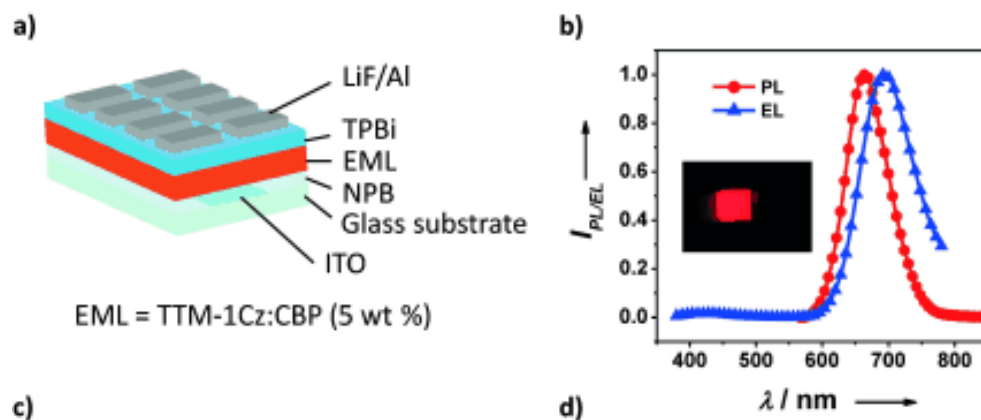


Figure 9. The PL and EL of the carbazole-TTM moiety.³⁹

1.3 Pnictogen Heteroles

Organic π -conjugated molecules have been extensively studied during the past 30 years; the interest in these compounds lies within their ability to display metal-like qualities such as conductivities similar to metals and semi-conducting properties.^{44 45} A diverse subsection of organic π -conjugated molecules is the heterole. The heterole is a molecular motif that has multiple structural advantages.⁴⁶ When compared to cyclopentadienide the introduction of various heteroatoms promotes the production of materials with tunable electronic properties. Although the introduction of heteroatoms into π -conjugated systems has obvious benefits, there were a few challenges that initially slowed progress in heavier main group element (E, where E= P, S, As, Sb, Te, etc.) based π -conjugated systems. These challenges include the high reactivity of E–C bonds due to increased bond polarity and weaker orbital overlap when large or electropositive E atoms

are present.⁴⁴ The typical heterole is composed of a butadiene fragment coupled to main group elements such as S, O, N, etc. This coupling involves interactions between the electron delocalization of the diene fragment and the lone pair of electrons on the heteroatom. The delocalization of electrons occurs when electrons in a π -conjugated molecule exchange across aligned p-orbitals of all neighboring atoms. When this occurs, the butadiene fragment and the heteroatom adopt a coplanar geometry. Additionally, the resonance of electrons causes the ground state of the molecule to lower, subsequently increasing the stability. As such, many of these heteroles are regarded as 6- π electron Hückel aromatic molecules.⁴⁴ The electronic properties of the heterole is dependent on the influence of the heteroatom and adjacent substituents. Examples of commonly known heteroles include in order: cyclopentadienide, pyrrole, furan, thiophene, and phosphole (Figure 10). Due to their tunable electronic properties, heteroles display attractive optoelectronic applications in organic electronic devices like OLEDs, OFETs, and OPVs^{46, 47}

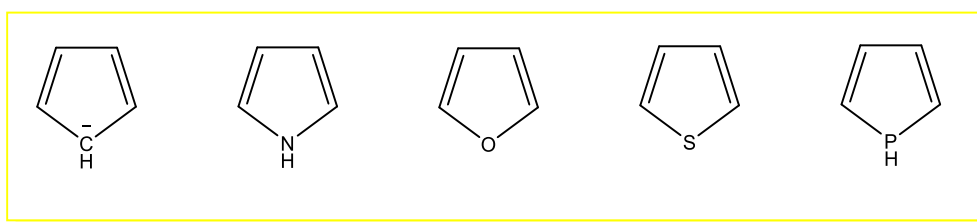


Figure 10. Cyclopentatdienide pyrrole, phosphole, furan and thiophene, five common heteroles.

In the realm of OLEDs, there is a niche of research that focuses on the use of carbazole as the π -conjugated heterole moiety. OLEDs are often composed of nitrogen rich units with sp^2 or sp^3 hybridized nitrogens;⁴⁷ as such, carbazole and its derivatives have been used extensively in OLEDs due to high thermal stabilities, high triplet energies

and efficient transportation of holes^{47, 48} The efficient transportation of holes is perhaps the most attractive feature of carbazole derivatives with respect to electro- and photoactive qualities. Many molecules used to produce blue or green emitting OLEDs contain carbazole derivatives which can be used as either an electron rich host or as an emissive layer.⁴⁹ Carbazole is considered a donor molecule and is therefore usually coupled to an electron withdrawing group (EWG) like an aromatic linking group or a π -conjugated inhibitor.⁵⁰ Despite carbazole's huge success in the OLED industry, not much research has been extended to other pnictogen (group 15) elements, such as phosphorus, arsenic, antimony, or bismuth.

When comparing pnictogen heteroles, it is important to note that nitrogen containing heteroles (*i.e.* carbazole and pyrrole) are the most unique. Since nitrogen is a second-row element, the lone pair of electrons in its 2p-orbital can overlap well with the π electrons in the butadiene fragment which are also delocalized using 2p orbitals. This overlap is what allows these heteroles to obtain aromaticity and therefore stability. Because the lone pair of electrons in nitrogen are housed in a 2p orbital, the orbital contains only one angular node and no radial nodes. The lack of radial nodes promotes easy overlap and planarization of the nitrogen and butadiene π systems. The expansion of p-orbitals of the phosphorus (3p) and arsenic (4p) atoms results in the introduction of radial nodes. These radial nodes inherent to p-orbitals of phosphorus, arsenic (and other heavy pnictogens) limit the overlap of the heteroatom lone pair with the butadiene π system by introducing increased antibonding interactions. This lack of overlap promoted by the larger atoms causes heavier pnictogen heteroles to behave more like cyclic 1,3-butadienes and/or pnictogen trihydrides (phosphine, arsines, or stibines).⁵¹ This behavior

causes the heavier heteroles to be much less aromatic than pyrrole. The orbital differences between pyrrole, phosphole and arsole can be seen in Figure 11. A DFT study was performed to determine the orbital compositions (B3LYP, Stuttgart RLC ECP for all atoms).⁵² For the phosphorus and arsenic analogues, a very small amount of aromaticity is reestablished through a hyperconjugation interaction between the π^* orbital of the pnictogen and the σ^* orbital of a substituent attached to the pnictogen.⁵³ To date, the most highly explored pnictogen containing pyrrole/carbazole derivative are a family of compounds known as phospholes.⁵⁴ Phospholes are beginning to be explored in organic electronic applications because of their high electron accepting and electron transporting capabilities.^{55, 56} Despite the significant lack of aromaticity compared to pyrrole or carbazole, the use of phospholes in organic materials has produced results comparable to the lighter counterpart.⁵⁷

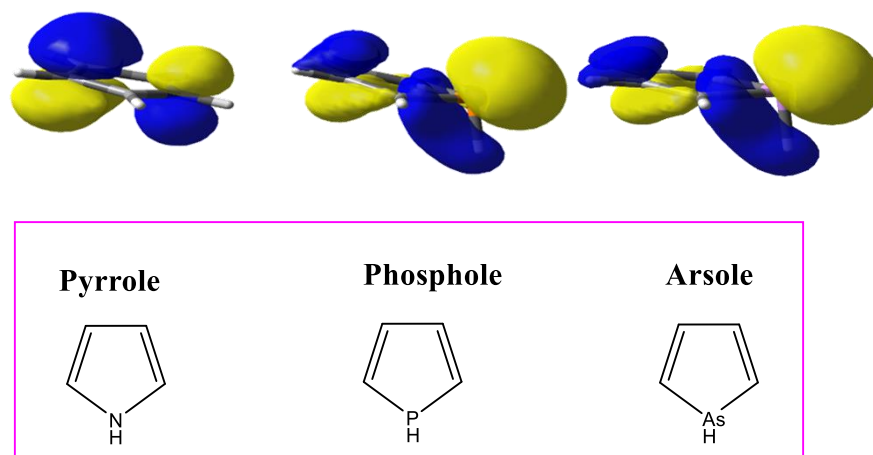


Figure 11. The HOMO diagrams of the pnictogen heteroles further confirm the pyramidalization of the heavier pnictogens. As the lone pair on the heavier atoms becomes more diffuse (due to the addition of radial nodes), the main group atom becomes more pyramidalized. Pyrrole is the most planar due to its lack of radial nodes and arsole is the most pyramidalized because of its 2 radial nodes.⁵²

2. RESEARCH MOTIVATIONS

2.1 Research Motivations

Motivated by recent results which incorporate carbazole moieties into emissive TTM radicals, the goal of the proposed research is to explore the effects of the introduction of other pnictogen-containing groups into the TTM radical system. Specifically, it is the goal to determine how the structure of the pnictogen-containing group influences the photophysical properties of the TTM radical. Through this research, it is expected that the following questions can be answered: Can the wavelength and therefore color of the emission be tuned? Can the quantum yield of the emission be improved or adjusted? Can the stability of these molecules be improved?

Any novel information obtained from this research will prove to be useful in the OLED industry. The OLED industry is currently flourishing yet there is still much to be discovered. Due to the exceptional reputation of carbazole, exploration of other pnictogen atoms can prove to be very beneficial. The heavier pnictogen analogs are less likely to be researched because of increased synthetic difficulties. This research program will focus specifically on the incorporation of phosphorus-containing moieties into TTM derived radicals for potential applications as OLED materials

2.2 Objectives

This thesis is comprised of the combination of several closely related projects, all of which involve the incorporation of pnictogen heteroles into the TTM radical system. Phosphorus derivatives were attempted first because phosphorus is the next heaviest pnictogen, and therefore, the chemistry of phosphorus should be the most similar to nitrogen in comparison to the other pnictogens. However, due to the addition of the radial

node in the 3p orbital of phosphorus atom, there are expected to be differences in their chemistry. The results can be expanded to the heavier pnictogens because each succeeding atom will contain an additional radial node that contributes to increased pyramidalization with decreasing delocalization. Any information obtained from the use of a phosphorus atom can be used to approximate information about heavier pnictogens.

Figure 12 shows the four dibenzophosphole compounds that were explored throughout the research. Compounds **1**, **3** and **4** are known molecules common in literature; compound **2**, however, has not been isolated. Diphenylphosphine derivatives **5-7** (Figure 12) were also incorporated into the research to serve as comparable data to the dibenzophospholes. The focus of the research will be placed mainly on molecules **2** and **5**, as they are the compounds that will be implemented into the TTM radical. Compounds **1,3** and **4** were synthesized as ways to get to compound **2** and compounds **6** and **7** were used throughout the experimental process simply for comparison reasons.

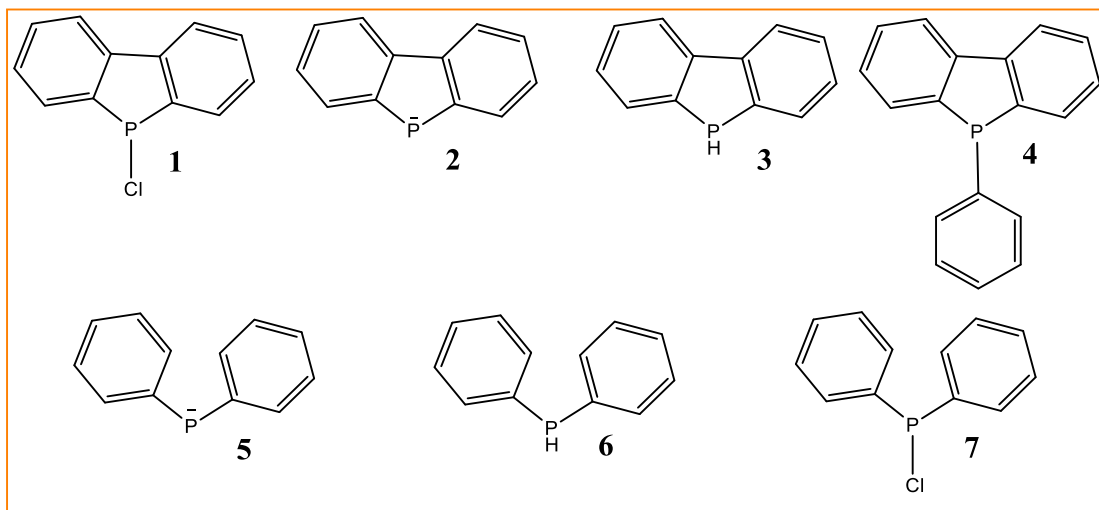


Figure 12. The dibenzophospholes and diphenylphosphines of interest

2.3 Spectroscopic and Analytical Tools Used for Characterization

The identity of the synthesized molecules was confirmed using heteronuclear

nuclear magnetic resonance (NMR) spectroscopy. Proton (^1H , referenced to residual solvent peak), phosphorus (^{31}P , referenced to external 85% H_3PO_4) and carbon (^{13}C , referenced to solvent peak) NMR were used extensively during the synthetic process because these tools yield information needed for direct structural analysis. ^{31}P NMR spectra were obtained as proton decoupled scans ($^{31}\text{P}\{^1\text{H}\}$) to prevent further complication of the spectral analysis resulting from phosphorus-proton spin coupling.

The identity of paramagnetic molecules was confirmed using electron paramagnetic resonance (EPR) spectroscopy which allowed for the determination of both the presence of unpaired electrons as well as for the elucidation of the of electronic environment of the electron.

3. DIBENZOPHOSPHOLE ANALOGS AND REACTIONS

3.1 Introduction

The immense benefits of the incorporation of the nitrogen atom in carbazole into emissive organic molecules has prompted the exploration of the remaining elements in the pnictogen group. This chapter will discuss the incorporation of the dibenzophosphole moiety, the phosphorus analog of carbazole. A study performed by Chen and Huang *et al.*, presented data on the optoelectronic properties of various substituted dibenzophosphole moieties (compounds and **A-J** in Figure 14).⁵⁷ Included in their data are calculated HOMO and LUMO estimates (Table 1). The calculated HOMO and LUMO levels of the specified dibenzophospholes were compared to the HOMO and LUMO levels of two known carbazole units, 9-methyl-carbazole (MeN) and 9-phenyl-carbazole(PhN); both carbazole units are commonly used in optoelectronic devices.⁵⁷ In comparison, the dibenzophospholes had lower HOMO and LUMO levels, but a wider range in energy gaps (E_g). The variation in gap levels is credited to the stronger electron donating ability of phosphorus compared to nitrogen.⁵⁸ The reported triplet energies (3E_g) of these dibenzophospholes also revealed their potential as host material.^{12 59}

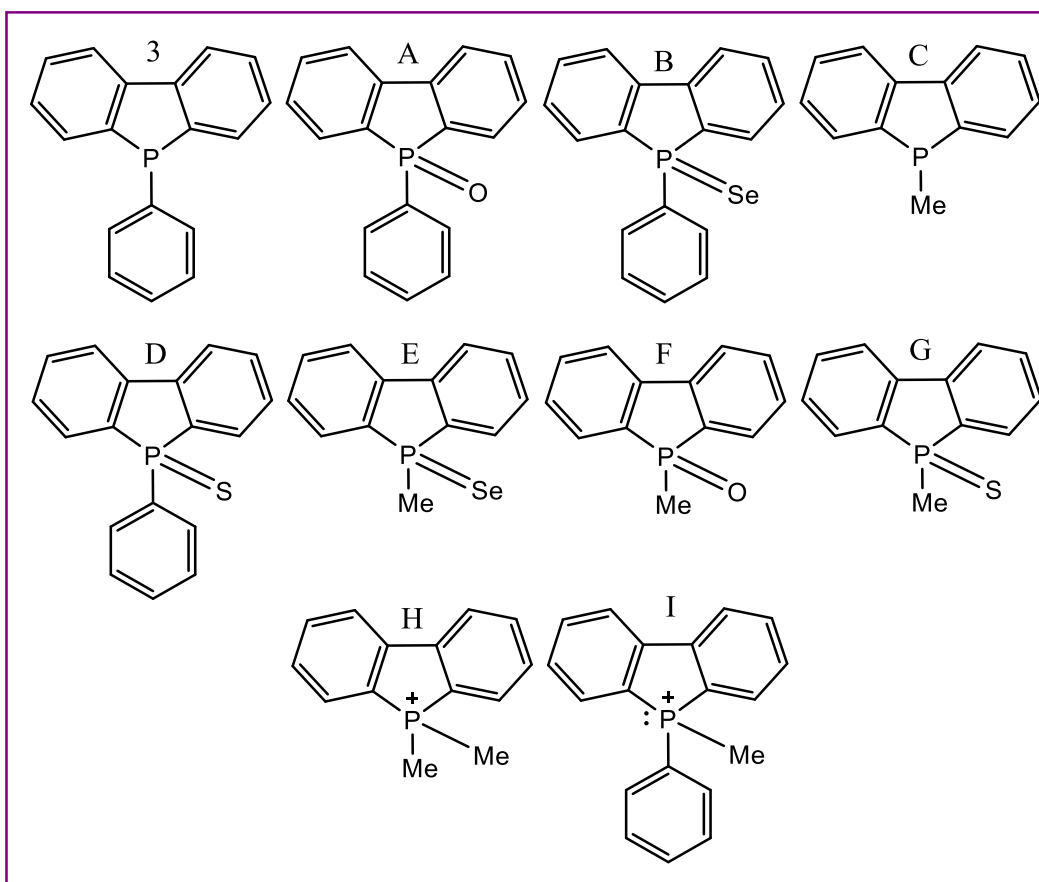


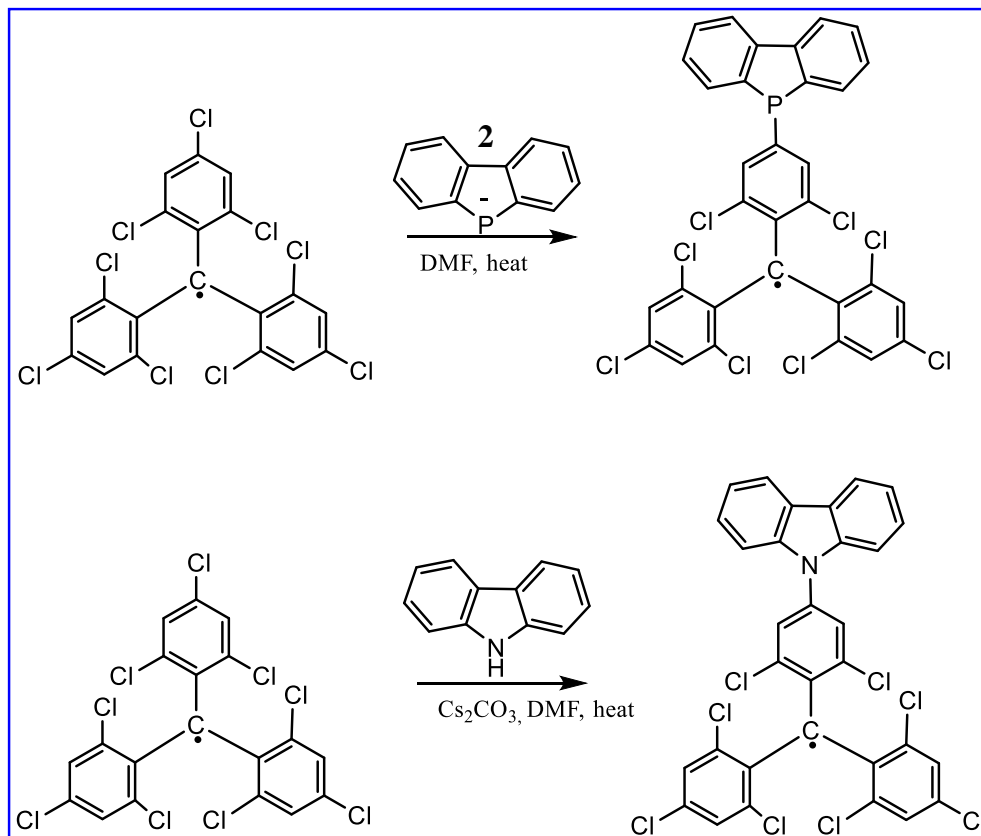
Figure 13. Prominent dibenzophospholes with optoelectronic properties.

Table 1. The HOMO, LUMO, band gap energies (E_g) and triplet energies (3E_g) of compounds 3, A-I as well as the MeN and PhN for comparison.⁶⁰

	3	A	B	C	D	E	F	G	H	I	MeN	PhN
HOMO	-5.9	-6.2	-5.5	-5.9	-5.9	-5.4	-6.3	-5.8	-	-9.6	-5.3	-5.3
O									9.8			
LUMO	-9.7	-1.5	-1.5	-9.8	-1.5	-1.6	-1.5	-1.6	-	-5.1	-6.2	-6.5
									5.3			
E_g	4.9	4.7	3.97	4.95	4.3	3.9	4.8	4.3	4.5	4.5	4.7	4.68
3E_g	2.9	2.8	2.2	2.95	2.8	2.2	2.8	2.8			3.18	

Chen and Huang et al. hinted at the benefits of electron withdrawing groups; a correlation between HOMO and LUMO levels showed that the incorporation of an electronegative group (in their case O,S, Se) increased the electron-transport ability of the dibenzophosphole.^{57, 60}

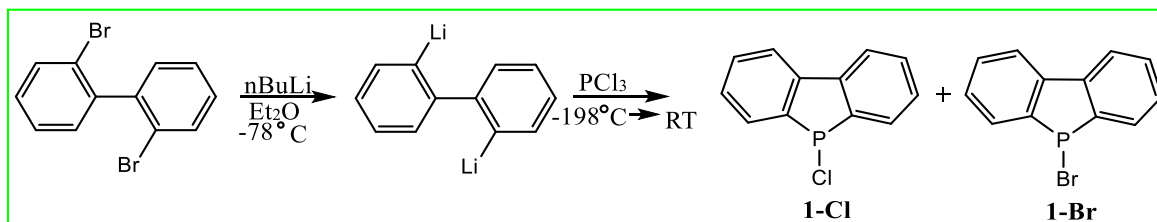
Inspired by the work of Chen and Huang, as well as the reports by Li and co-workers, the first goal of this thesis research was to incorporate a dibenzophosphole group into the TTM radical in place of carbazole. Although there is less aromaticity in the dibenzophosphole unit, it is still expected to change the optoelectronic properties of the resulting radical. The first attempt at installing the dibenzophosphole was pursued in the same fashion as the carbazole by the generation of the dibenzophospholide anion (**2**) (Scheme 1). The electron density on the phosphorus promotes the donation of electrons onto the para carbon of one of the three aromatic rings in the TTM system. The mechanism involves a nucleophilic aromatic substitution; a chloride atom from the para position is displaced readily allowing for the incorporation of nucleophiles.



Scheme 1. The addition of the dibenzophospholide into the TTM system (top) and reported installation of carbazole into TTM (bottom).³⁷

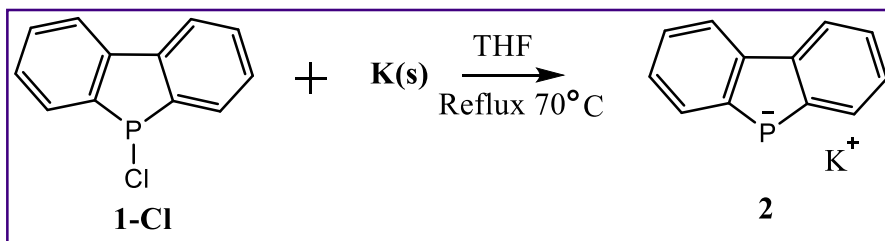
3.2 Synthesizing dibenzophospholes

The chlorophosphole (**1**) was the first compound synthesized. The halo-dibenzophosphole was chosen as the first target compound because halogen substituents can be readily reduced to give phosphorus centered anions, making it easier to reach the desired phospholide product.⁶¹ The synthesis used to make this product can be seen in Scheme 2.



Scheme 2. Synthesis of Chlorodibenzophosphole

In its purest form the chlorophosphole (**1-Cl**) product was a pale-yellow solid with an apparent sand-like texture. After synthesizing the product, its identity was confirmed by NMR. The ^{31}P NMR yielded a product peak at 68.15 ppm, which is consistent with the literature and falls in the expected chemical shift range for halogenated phosphorus compounds (35-200ppm).^{62 63} As the phosphorus atom becomes more electron deficient, the nucleus becomes deshielded and resonates downfield at a more positive chemical shift. The synthesis of **1** also results in the generation of a significant side product, namely the bromophosphole (**1-Br**), which exhibits an ^{31}P NMR chemical shift of 49.21 ppm.⁵⁷ The formation of this byproduct has been reported in the literature,⁶¹ and can be rationalized as the 2,2'-dibromobiphenyl starting reagent serves as a source of bromine during the synthesis of **1**. These two different products form in a 3:2 chlorine to bromine ratio, yet their separation is not necessary. Both P-X (X = Cl or Br) bonds exhibit analogous reactivity; therefore, using the mixed product for further synthesis should not be detrimental. The relative purity of the product mixture was affirmed via ^1H NMR. The compound contains 4 protons on each benzene ring making a total of 8 aromatic protons. Although the nuclear spins of phosphorus and hydrogen are the same ($I = 1/2$), there is no significant ^1H - ^{31}P coupling seen in the ^1H NMR. To prepare the phospholide anion, the mixture of compounds **1-Cl** and **1-Br** were treated with a potassium mirror in refluxing THF (Scheme 3). The P atom of phospholide anion is much more reactive compared to the P atom in the **1** due to its negative charge, and therefore should be more reactive in the desired nucleophilic aromatic substitution reaction with the TTM radical.

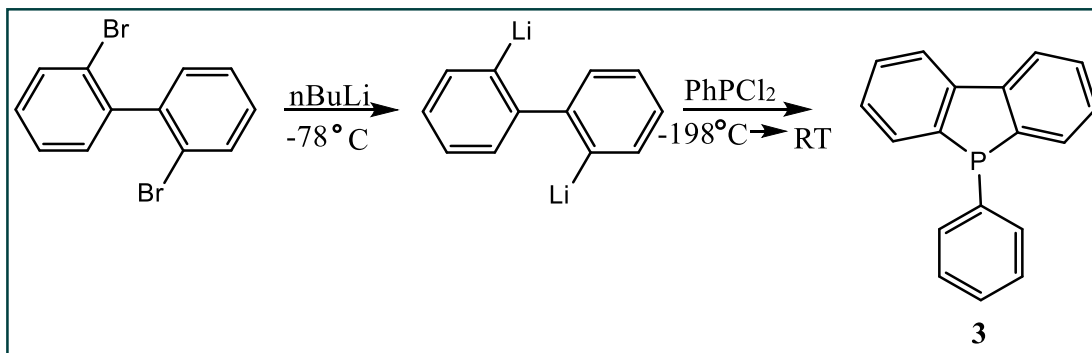


Scheme 3. Synthesis of potassium dibenzophospholide ($[K^+][2]$)

The 1H NMR of the phospholide anion was very similar to the spectra obtained for product **1-Cl**, however there is a stark difference in the ^{31}P NMR. The initial 68.15 ppm peak in **1-Cl** was shifted upfield to -21.01 ppm. This large shift is due to the presence of the negative charge on the P atom causing it to be shielded by electron density. Although the dibenzophospholide has not been isolated and characterized in scientific literature, the ^{31}P peak obtained correlates with the expected shift of a molecule with a phosphide anion (for example the phosphorus atom in diphenylphosphide resonates at -12.9 ppm).⁶¹

We next focused on the synthesis of the *P*-phenyl-dibenzophosphole (**3**) (Scheme 4) which could also be used to generate the diphenylphospholide anion **2**. The synthesis of this phosphole is reminiscent of the synthesis of product **1**, the only difference being that dichlorophenylphosphine was used in place of PCl_3 to introduce the phosphorus moiety. **3** was identified as a sticky off-white solid, with a ^{31}P NMR chemical shift at -10.35 ppm.⁶⁴ The influence of the substituent on the P atom is apparent when comparing the ^{31}P NMR of **1** and **3**, the less electronegative aryl group in **3** results in a less deshielded phosphorus center when compared to that in **1**. The 1H NMR only exhibited peaks in the aromatic region; the same 8 protons from the product **1** are seen along with an additional 5 protons from the phenyl ring. The 5 protons from the phenyl group

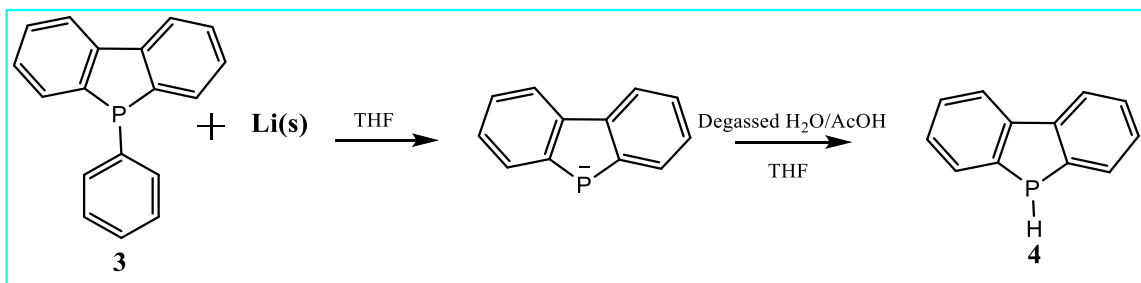
produce peaks more upfield compared to the 8 protons in the dibenzo system because they are slightly shielded.



Scheme 4. Synthesis of Phenyldibenzophosphole

The dibenzophospholide (**2**) was also synthesized using **3**. Instead of using potassium, the phenyl substituent was removed using lithium granules. Much like the dibenzophospholide synthesized from the **1**, this lithium phospholide exhibited a ^{31}P peak at -21 ppm. Given the negative charge on the P in the phospholide, it is reasonable to assume that the subsequent peak would occur upfield and in the negative region of the spectrum. As previously mentioned, the dibenzophospholide has never been isolated so the legitimacy of the product was further confirmed via comparison to potassium diphenylphosphide, which is a known compound that is structurally similar to the dibenzylphospholide product. Potassium diphenylphosphide exhibits a ^{31}P peak at -12.9 ppm, and therefore it can be assumed that the product synthesized with a ^{31}P NMR signal at -21.29 ppm is indeed the expected phospholide anion.⁶⁵ Although there is a large chemical shift difference between these two compounds, the phospholide anion was expected to produce a more upfield peak compared to the phosphide because the heterole confirmation promotes more electron donating from the benzene rings into the phospholide atom.

Finally, we also synthesized dibenzophosphole (**4**) from **3** (Scheme 4) as an additional potential starting material for introduction into the TTM radical. The P-phenyldibenzophosphole was stirred over Li granules to make the phospholide, which was subsequently protonated using degassed water and acetic acid to give the dibenzophosphole product.⁴⁵



Scheme 4. Synthesis of dibenzophosphole

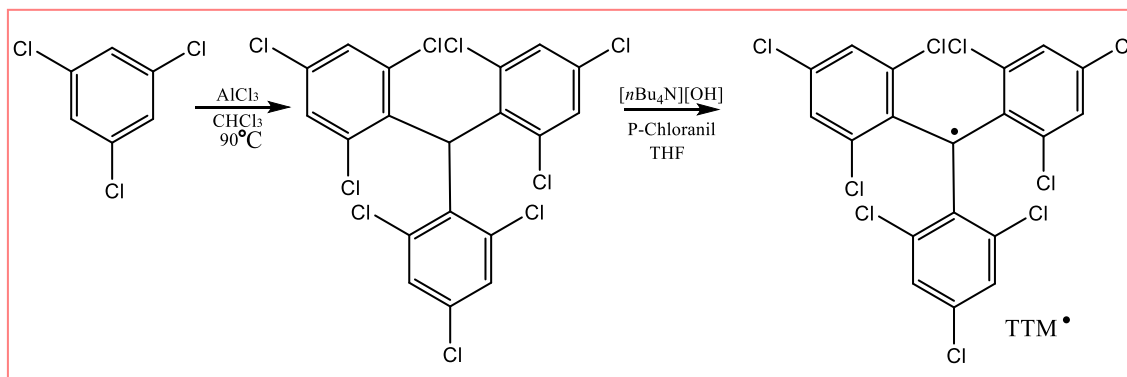
Much like the other phosphole products, the identity of compound **4** was confirmed through ³¹P and ¹H NMR spectroscopies. The ¹H NMR yielded the typical 8 aromatic protons found in the dibenzo system along with what seems like two singlets in the 5-6 ppm range. There is only one additional proton in the structure, so there should only be one additional singlet corresponding to the hydrogen attached the P atom. Interestingly, what looked like two singlets in the ¹H NMR spectrum of **4** was actually one doublet with a large coupling constant of 200 Hz which was attributed to a one-bond ³¹P-¹H coupling. To confirm this assignment, the ¹H coupled ³¹P spectrum also yielded a doublet with a ¹J_{P-H} = 198 Hz and confirmed the presence of a bond between the P atom and its H substituent. The coupling constants were measured using the following equation:

$$J_{(\text{Hz})} = \Delta_{\text{ppm}} \times \nu \quad (1)$$

where Δ_{ppm} is the chemical shift difference between the peaks of interest and ν is the resonance frequency of the nucleus being interrogated.

3.3 Addition of Dibenzophospholide into the TTM system

The synthetic process involved in attaching the dibenzophospholide to TTM can be reviewed in Scheme 1. Theoretically, the phospholide should replace one of the chlorine atoms and assist in the stabilization of the radical. First, the TTM was obtained first through a Friedel-Crafts alkylation of trichlorobenzene using chloroform as the alkylating agent and aluminum trichloride as a Lewis acid. This reaction produces HTTM, which is the H substituted TTM molecule. The synthetic process can be seen in Scheme 5. The radical was then generated by first deprotonating the triarylmethyl C-H group using tetra-*n*-butyl ammonium hydroxide ($[n\text{-Bu}_4\text{N}][\text{OH}]$) followed by oxidation of the resulting triaryl anion using *p*-chloranil.



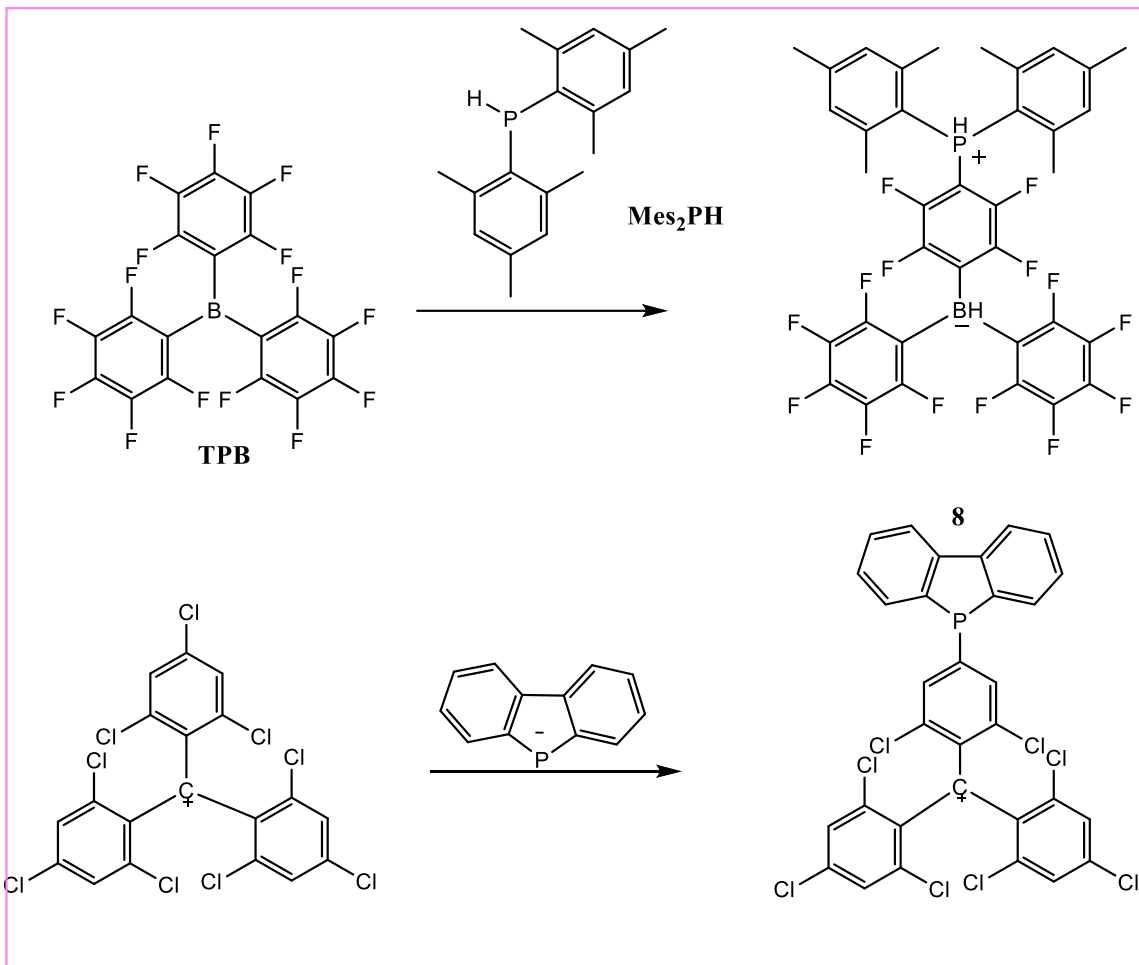
Scheme 5. Synthesis of TTM radical

The TTM radical is a bright red solid that fluoresces bright orange. Paramagnetic molecules are not NMR active because they reduce relaxation times which contribute to very broad peaks in the NMR. Consequently, the validity of the radical was confirmed via EPR. The spectrum yielded one radical peak, indicating that there were no coupling

interactions.

Once the TTM radical was synthesized and characterized, efforts were made to attach the dibenzophospholide anion to the system. Although the synthesis used was very similar to the synthesis involved in attaching carabazole to TTM, the installation of the dibenzophospholide moiety into the TTM radical was unsuccessful. All data obtained from these experiments indicated that once the phospholide was added, the TTM radical reverted into the protonated starting material, HTTM, which contains a closed shell, diamagnetic system rather than the desired radical.

As previously mentioned, the TTM radical is an air stable open shell system that produces deep red emissions. The paramagnetic radical is preferred due to the open shell system having theoretical maximum a quantum efficiency of 100%; however, due to the difficulty of adding the dibenzophospholide directly to the TTM radical, the same chemistry was attempted with the known TTM cation (TTM⁺).⁶⁶ It was anticipated that TTM⁺ would be more reactive than the TTM radical toward nucleophilic aromatic substitution with the phospholide anion. The nucleophilic addition of phosphorus to TTM⁺ was also inspired by chemistry developed by Stephan and co-workers where dimesitylphosphine (Mes₂PH, Mes = 2,4,6-trimethylphenyl) was added to tris(pentafluorophenyl) borane (TPB) using nucleophilic aromatic substitution.^{67, 68} Given that carbocations are isoelectronic and isolobal to boranes, it was assumed that similar chemistry could be carried out using dibenzophospholide and TTM⁺ (Scheme 6).



Scheme 6. Addition of Mes_2PH to TPB as reported by Stephan,⁶⁷ and attempted addition of dibenzophospholide to TTM^+ .

TTM^+ was synthesized from the TTM radical by oxidation in chlorinated solvents using antimony pentachloride (SbCl_5) as an oxidant.⁶⁶ Using this synthetic methodology, the resulting cation is balanced with the counter anion SbCl_6^- . The $[\text{TTM}][\text{SbCl}_6]$ is a dark blue solid and its purity was confirmed through ^1H NMR before further use.

The addition of **2** to the TTM^+ resulted in a sticky red solid with orange fluorescence. The ^{31}P NMR yielded a peak at 41.40 ppm; peaks in this range indicate that the phosphorus atom in the molecule is attached to an electron withdrawing group. The phosphorus atom is bound through a phenyl ring, which are typically electron donating

groups when unsubstituted, however in this case the phenyl ring can be viewed as electron withdrawing because of its electronegative chloro substituents and cationic nature. The ^{31}P NMR also produced another significant peak at 67.99 ppm; this peak is reminiscent of the chlorophosphole, which indicates that this byproduct may have been formed throughout the reaction. This by product is unfortunately the major component of the product mixture based on the integration of the peak (1.00) relative to the 41.40 ppm product peak (0.08).

3.4 Experimental

Dichlorodibenzophosphole (1) 2.49g (7.98 mmol) of dibromobiphenyl was dissolved 50 mL of anhydrous diethyl ether (Et_2O) and added to a 100 mL Schlenk flask. The solution was cooled then placed into an ice bath until it was cooled down to 0°C . 10.0 mL of n-Butyllithium (1.6M, 16 mmol) was added dropwise to the mixture which caused the clear solution to adopt a pale-yellow color. The solution was left to stir at room temperature for approximately 1 hour before it was then cooled back down to -198°C using liquid N_2 . Phosphorus trichloride (PCl_3) (5.0mL, 52.2 mmol) was added dropwise to the frozen mixture. Once all the PCl_3 was added, the flask was left to warm up to room temperature while stirring. The solution was left to stir for 15 minutes, after which a white precipice began to form. Volatile materials were removed *in vacuo* and the resultant residue was left to dry under vacuum for 1 hour. The desired product was obtained after it was extracted via two toluene extractions. ^1H NMR (400 MHz, CDCl_3) δ 7.30 – 7.35 (m, 2H), 7.39 – 7.42 (m, 2H), 7.65 – 7.71 (m, 2H), 7.91-8.0 (d, 2H). ^{31}P NMR (162 MHz, C_6D_6) δ 49.21 (s), 68.15 (s).

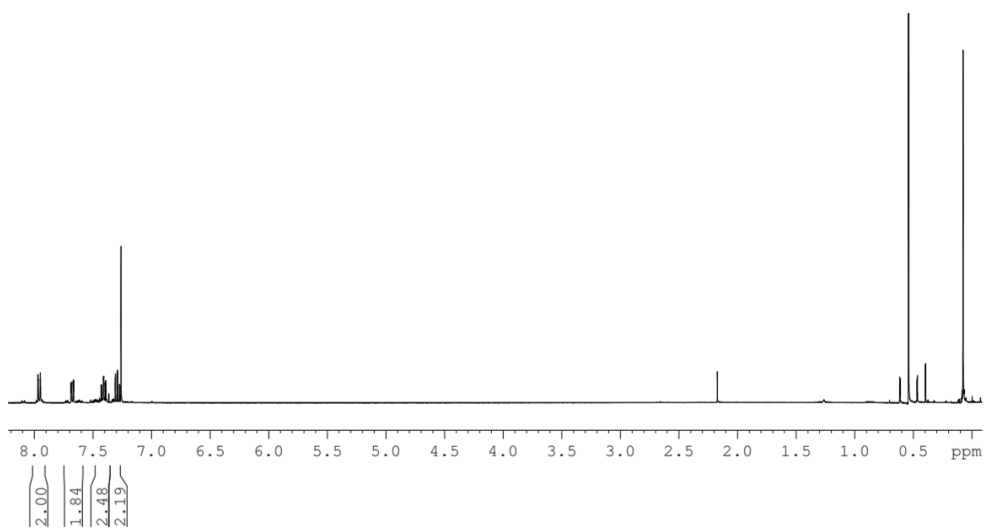


Figure 14. Product 1 ^1H NMR spectrum in CDCl_3 .

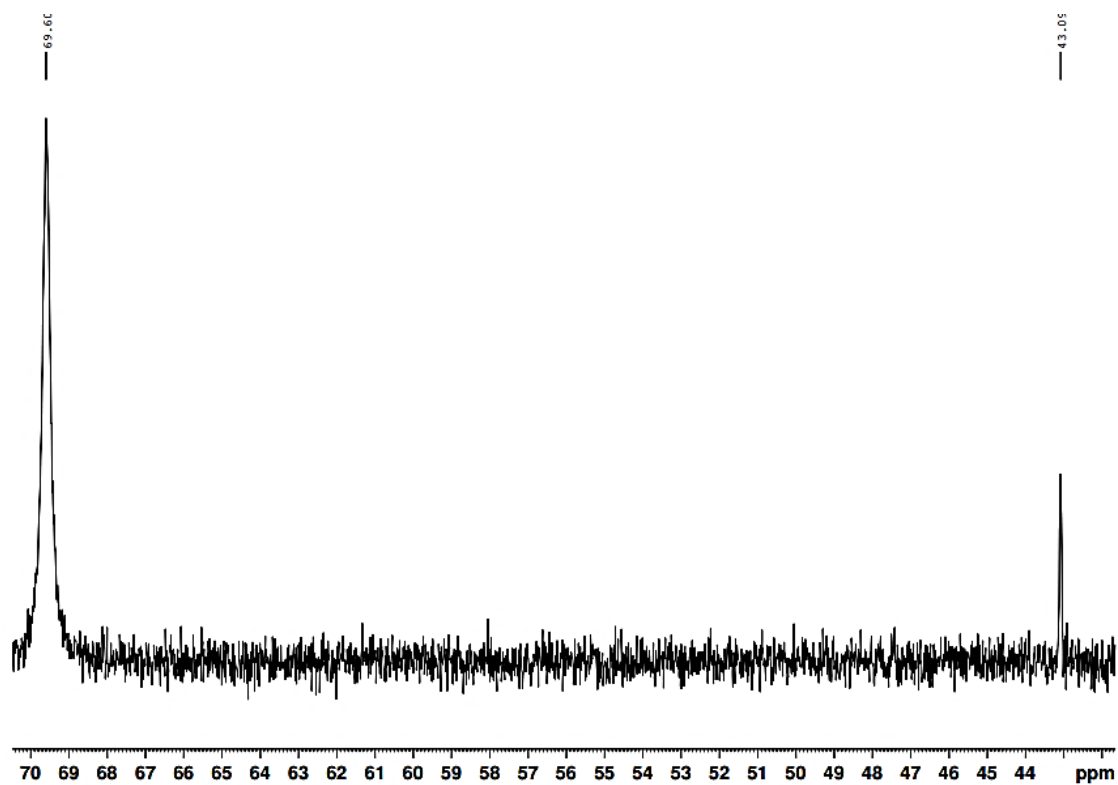


Figure 15. Product 1 ^{31}P NMR spectrum in CDCl_3 .

Potassium dibenzophospholide ([K][2]) In a nitrogen-filled glove box, 0.1369g (3.47mmol) of potassium metal was placed inside a 50 mL Schlenk flask. The Schlenk

flask was removed from the glove box and heated with heat gun to melt the K until it formed a mirror around the sides of the flask. The flask was taken back into the glove box and 0.640g (2.91mmol) of **1** dissolved in 20 mL of anhydrous THF was added dropwise into the Schlenk flask. The solution was refluxed at 70°C for 16 hours. The solution was then cooled and filtered to remove unreacted K metal. The solvent was removed *in vacuo*. The product was a pale yellow solid. ¹H NMR (400 MHz, C₆D₆) δ 7.42 – 7.33 (m, 1H), 7.07 – 6.99 (m, 1H), 6.99 – 6.93 (m, 1H), 6.83 (dddd, *J* = 8.8, 7.5, 2.7, 1.6 Hz, 1H). ³¹P NMR (162 MHz, C₆D₆) δ -21.93 (s).

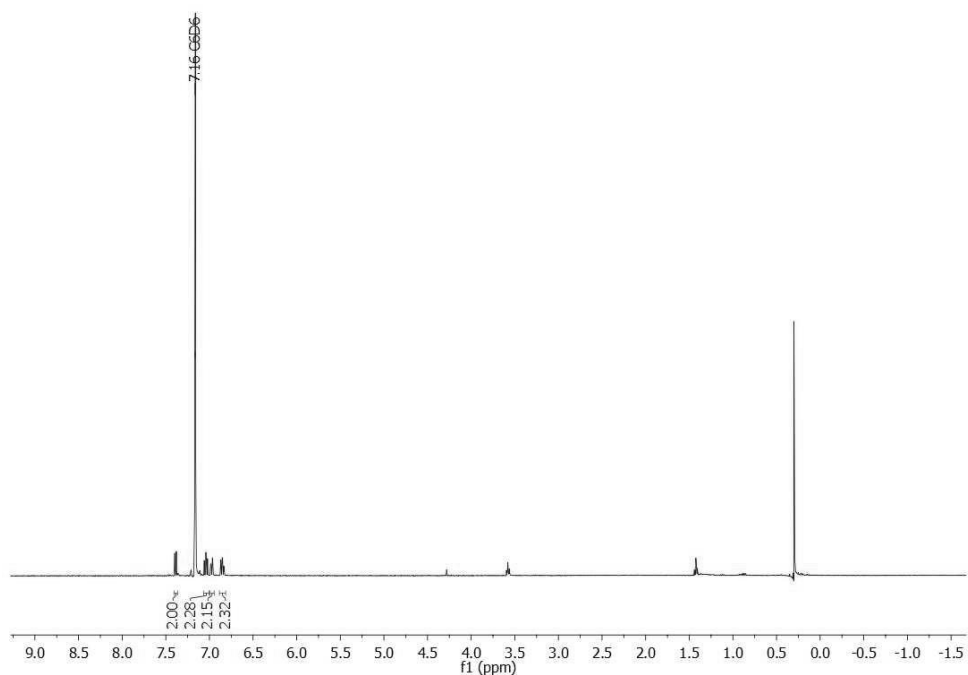


Figure 16. Product **[K][2]** ¹H NMR spectrum in C₆D₆.

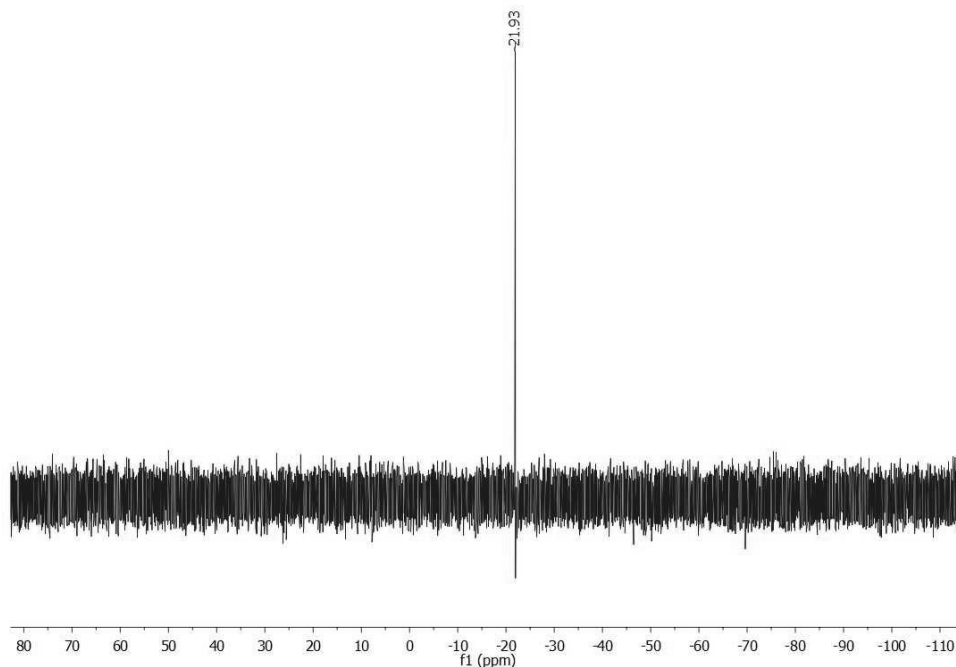


Figure 17. Product **[K][2]** ^{31}P NMR spectrum in C_6D_6 .

***P*-phenyldibenzophosphole (3)** Approximately 0.60g of dibromobiphenyl (2 mmol) was dissolved in 10 mL of anhydrous tetrahydrofuran (THF) in a 25 mL Schlenk flask. The solution was allowed to stir for 10 minutes before it was cooled to -78°C using an acetone a dry ice bath. 1.52 ml (4 mmol, 2.57 M) of n-butyllithium was added dropwise to the cooled mixture. The solution was allowed to stir for 30 minutes. 0.34g (2 mmol) of dichlorophenyl phosphine (PhPCl_2) was dissolved in 1 mL of THF was then added by syringe into the di-lithiated biphenyl solution. The yellow mixture warmed up to room temperature while it was left to stir overnight. The next day the volatile solvents were removed *in vacuo* and a honey colored oil was left over. The product was extracted from this oily material with dichloromethane (DCM) and then filtered over a plug of celite and silica gel. The entire solution was concentrated under vacuum and the product was removed from an oily solution via recrystallization using degassed methanol. ^1H NMR

(400 MHz, CDCl₃) δ 7.96 (d, J = 7.9 Hz, 1H), 7.76 – 7.63 (m, 1H), 7.47 (td, J = 7.6, 1.2 Hz, 1H), 7.33 (ddd, J = 11.2, 6.4, 1.6 Hz, 2H), 7.25 – 7.20 (m, 1H). ³¹P NMR (162 MHz, CDCl₃) δ -10.94 (s).

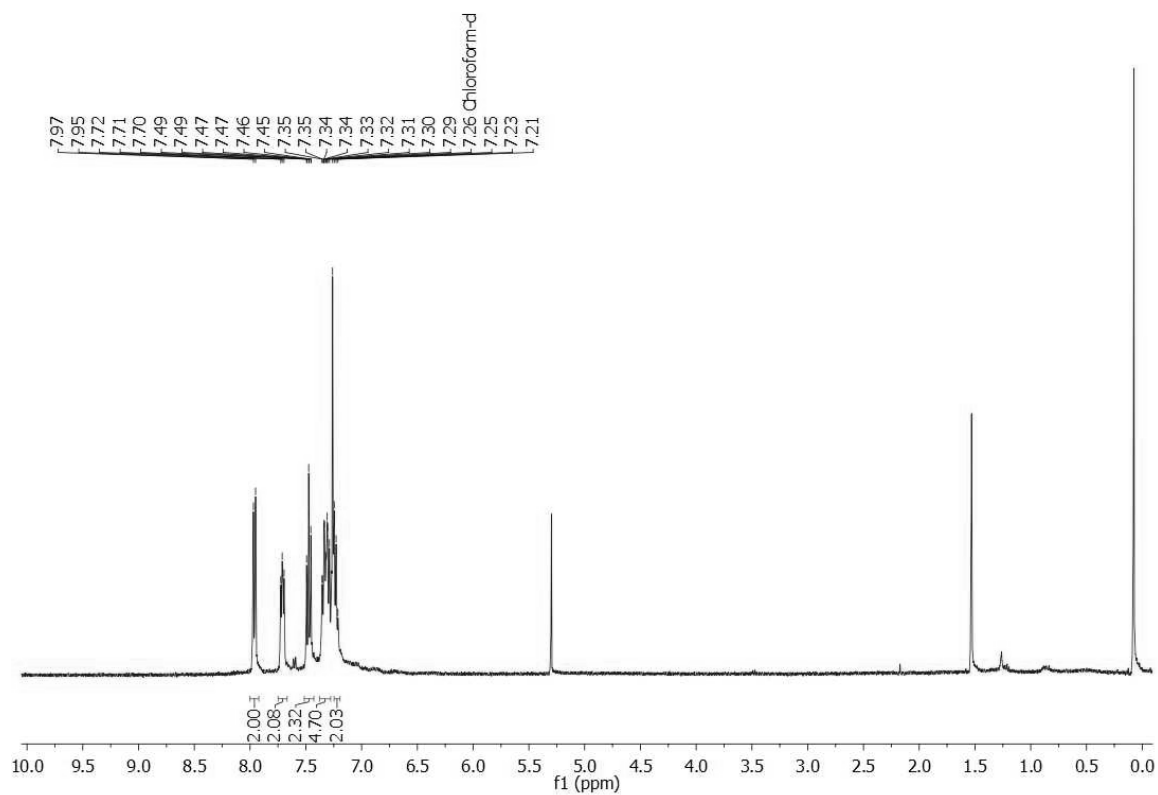


Figure 18. Product **3** ¹H NMR spectrum in CDCl₃.

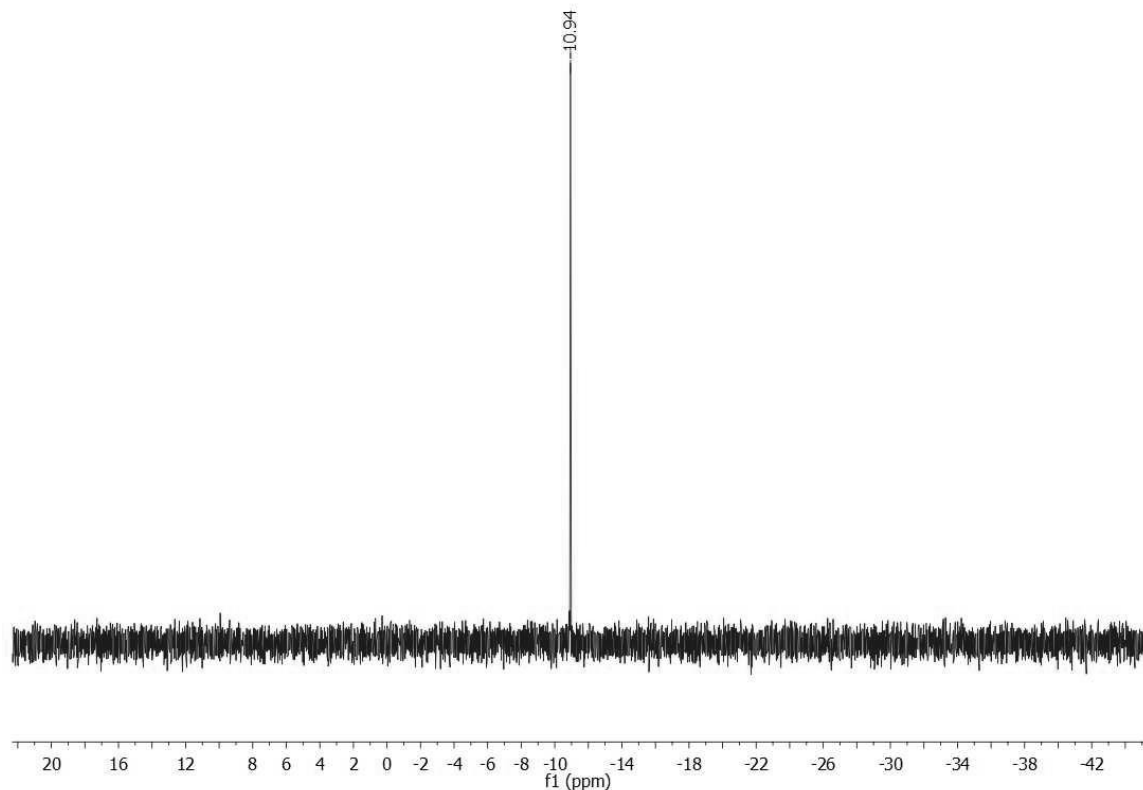


Figure 19. Product **3** ^{31}P NMR spectrum in CDCl_3 .

Dibenzophosphole (4) 0.305g of **3** (1.17 mmol) was combined with 0.0081g of lithium (Li) metal in a 25 mL Schlenk flask. 10mL of THF was added to the compounds and the resultant solution was left to stir for 4.5 hours. After stirring for the allotted time, the solution was canula transferred into another Schlenk flask to separate it from unreacted Li metal. An aliquot of a degassed H_2O (1.5mL)/AcOH (0.4mL) solution was added to the reaction mixture. The entire solution was then placed under vacuum to remove volatile solvents. The product was separated from unwanted products by extracting with DCM and subsequent air-free filtration over a plug of dry alumina. The resultant white powder was further washed with anhydrous pentane. ^1H NMR (400 MHz, C_6D_6) δ 7.73 – 7.67 (m, 2H), 7.22 – 7.18 (m, 1H), 7.07 – 6.99 (m, 3H), 6.93 – 6.89 (m, 2H), 5.17 (d, $J = 197.4$ Hz, 1H). ^{31}P NMR (162 MHz, CDCl_3) δ -67.98 (s).

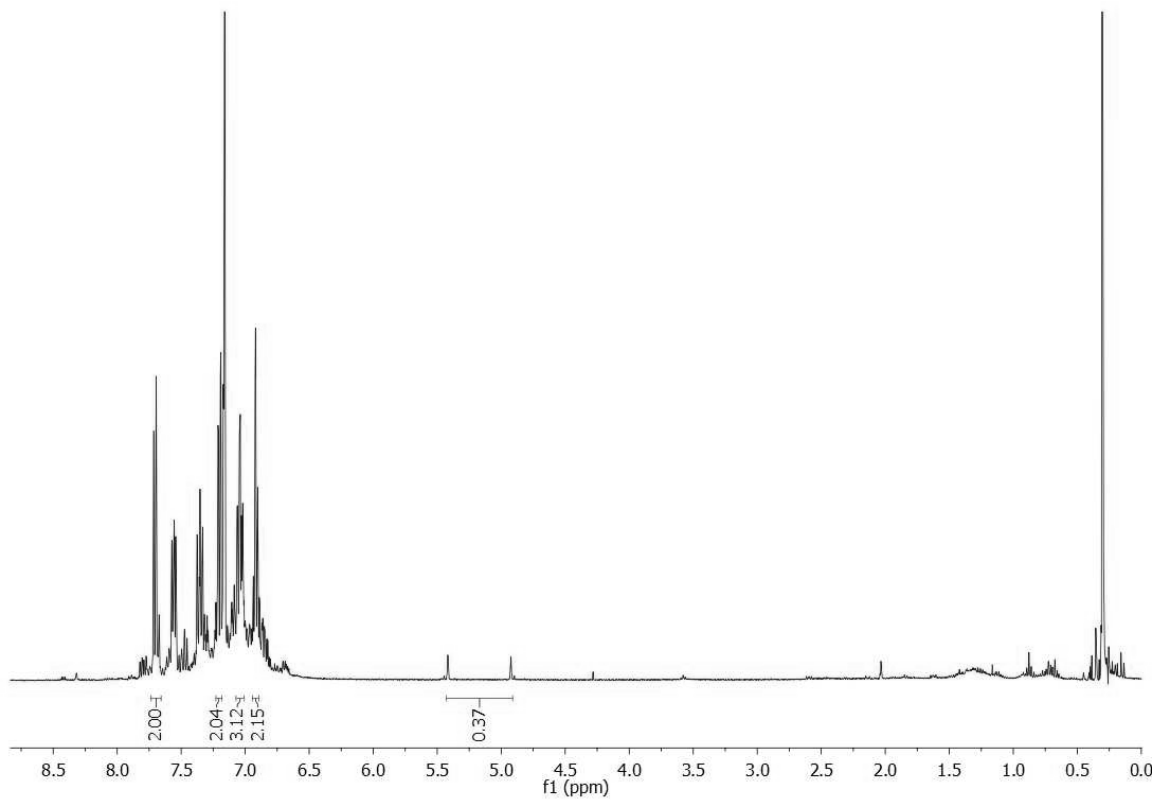


Figure 20. Product 4 ^1H NMR spectrum in CDCl_3 . (Product contained excess starting material)

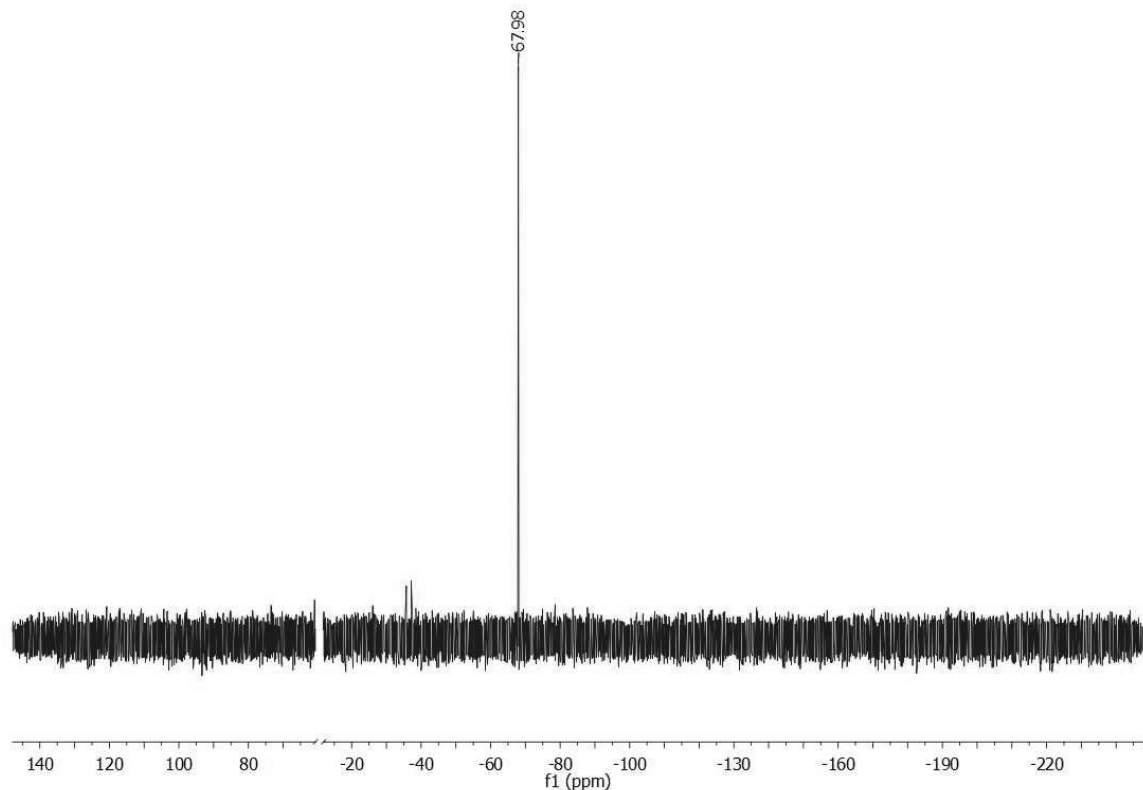


Figure 21. Product **4** ^{31}P NMR spectrum in CDCl_3 .

HTTM 1.0g (5.5 mmol) of trichlorobenzene (TCB) was placed into a 50 mL pressure flask inside a nitrogen-filled glovebox. 0.073g (0.612 mmol) of chloroform (CHCl_3) was added into the flask followed by 0.074g of anhydrous aluminium trichloride (AlCl_3). The mixture was stirred and heated to 85°C for 2 hours. The solution was then cooled to 25°C and 20 mL of 0.1N HCl was added into the solution in an ice bath. The resulting yellow solution was extracted with 50mL of CHCl_3 . The organic layer was then dried over magnesium sulfate for an hour and then filtered. The subsequent solution was concentrated using a rotary evaporator. The product was identified as an off-white solid that was further washed with hexane to produce a white solid. ^1H NMR (400 MHz, C_6D_6) δ 6.99 – 6.97 (m, 1H), 6.93 – 6.91 (m, 1H), 6.76 (s, 1H).

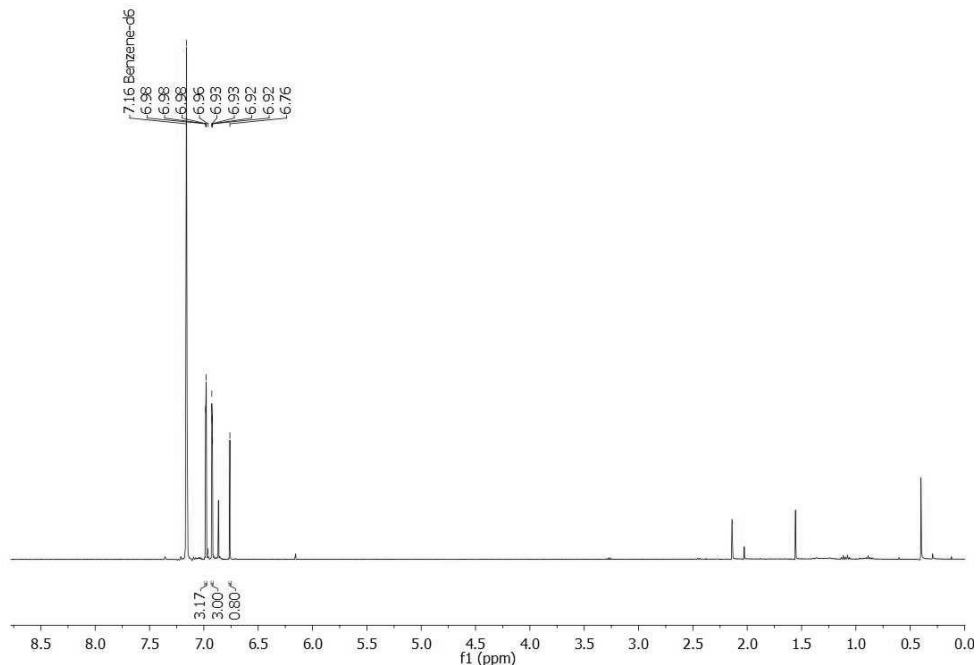


Figure 22. HTTM ^1H NMR spectrum in C_6D_6 .

TTM In nitrogen filled glove box, 3.0g (5.41 mmol) of HTTM was placed into a Schlenk flask previously wrapped in aluminum foil. 4.60 mL of n-butylammonium hydroxide (4.56g, 7.03 mmol) in 50 mL of THF was combined with the HTTM contained in the Schlenk flask. Upon combination the solution turned a deep red color. The solution was left to stir for 4 hours, after which 1.86g (7.57 mmol) of p-chloranil in 25 mL of THF was syringe transferred into the solution. The mixture was left to stir overnight, and the resultant purple solution was concentrated *in vacuo*. The dark purple solid was mixed with 1.0g of silica gel in 10 mL of DCM. The solid was again concentrated under vacuum. The product was purified via a packed silica gel column and 100% hexanes the eluent.

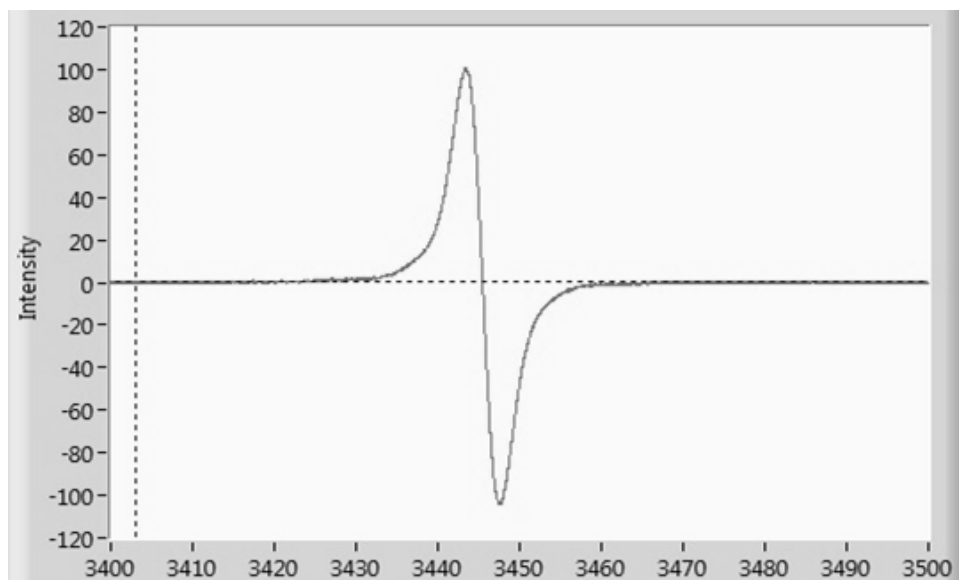


Figure 23. TTM radical EPR spectrum, where the x-axis presents the g-factor and the y-axis corresponds to the intensity.

TTM⁺SbCl₆⁻ (6) In a nitrogen filled glove box, a 50mL Schlenk flask covered with aluminum foil was charged with 0.5024g (0.907mmol) of TTM radical and 0.5510g (1.841mmol) of SbCl₅. The Schlenk flask was removed from the glove box and 20mL of CCl₄ was syringe transferred into the flask. The solution was left to stir over night, after which solvent was removed *in vacuo*. The solid obtained was dark blue. ¹H NMR (400 MHz, CDCl₃) δ 7.37 – 7.35 (m, 3H), 7.24 – 7.22 (m, 3H).

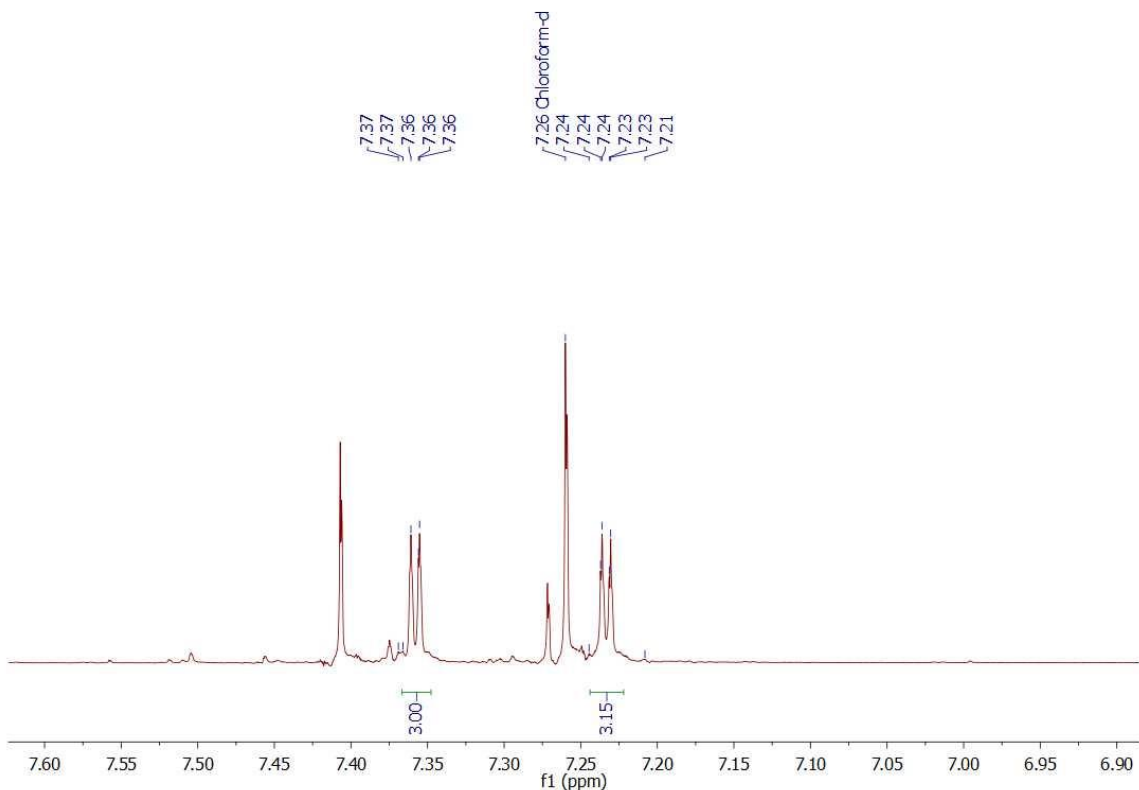


Figure 24. Product **6** ^1H NMR spectrum in CDCl_3 . The peaks at 7.40ppm and 7.27ppm represent impurities.

TTM+P(8). In a nitrogen filled glovebox, 0.2235g (0.253mmol) of product **6** was placed in a 25mL Schlenk flask covered with aluminum foil 10mL of anhydrous THF was also added into the flask. 0.0513g (0.225mmol) of **2** was dissolved in 3mL of THF and then subsequently added dropwise into the flask. The initially dark blue color of the solution turned bright red upon addition. The solution was allowed to stir over night. The THF was removed *in vacuo* and the resultant product was a sticky red substance with orange fluorescence. ^1H NMR (400 MHz, C_6D_6) δ 7.54 (d, $J = 6.9$ Hz, 1H), 7.32 (d, $J = 7.6$ Hz, 1H), 7.05 (t, $J = 7.1$ Hz, 1H), 6.93 (t, $J = 7.3$ Hz, 1H). ^{31}P NMR (162 MHz, C_6D_6) δ 41.40 (s).

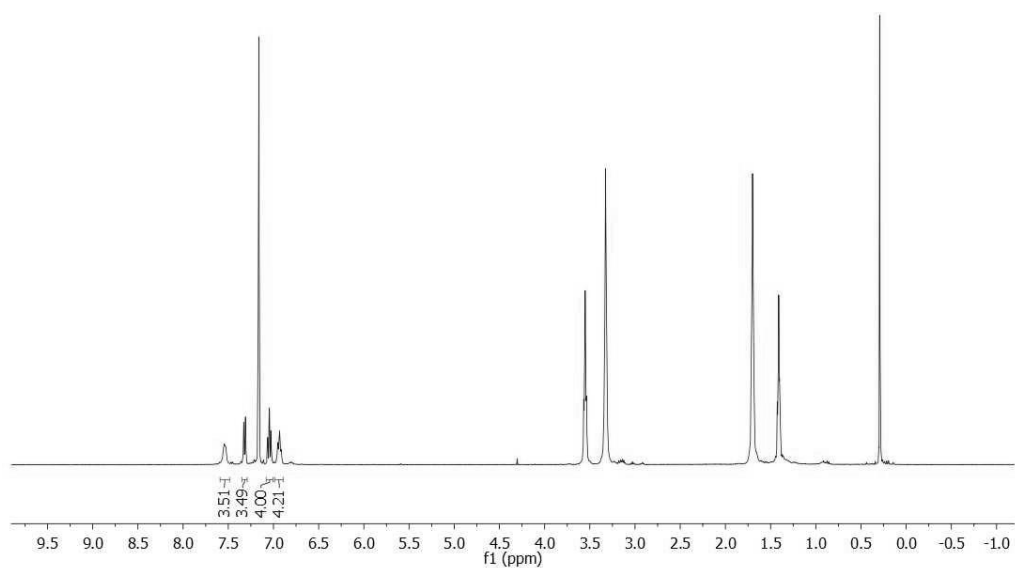


Figure 25. Product **8** ^1H NMR spectrum in C_6D_6 .

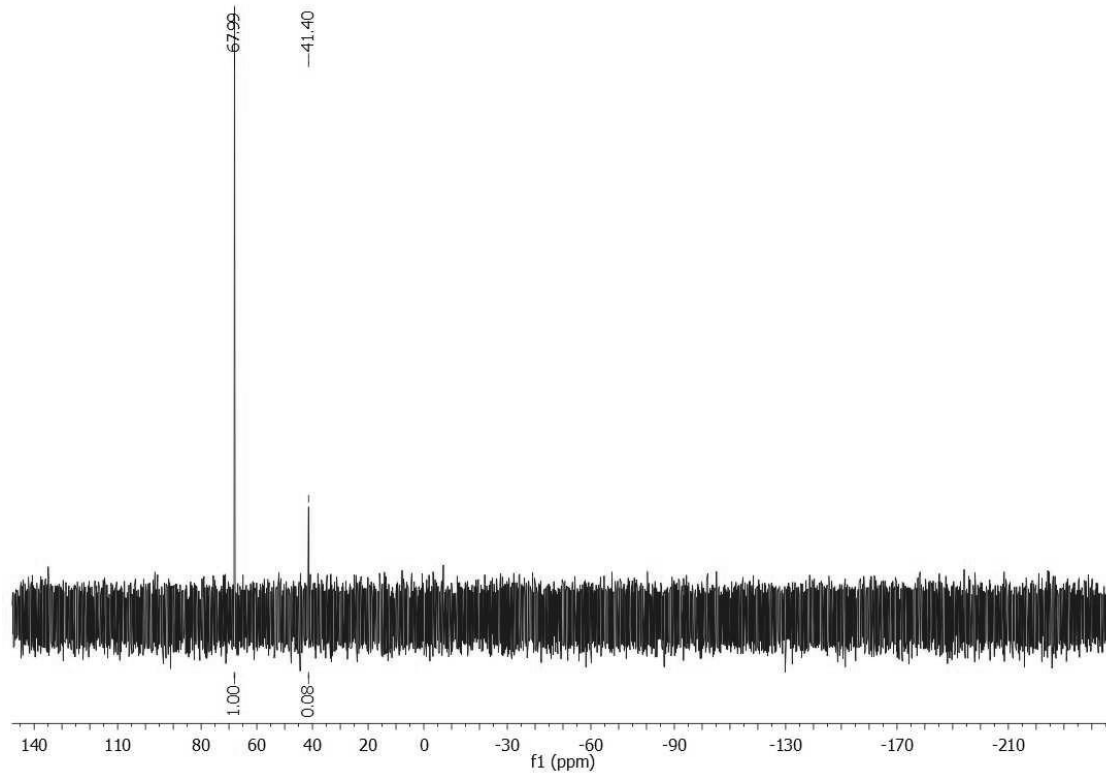


Figure 26. Product **8** ^{31}P NMR spectrum in C_6D_6 .

4. DIPHENYLPHOSPHINE ANALOGS AND REACTIONS

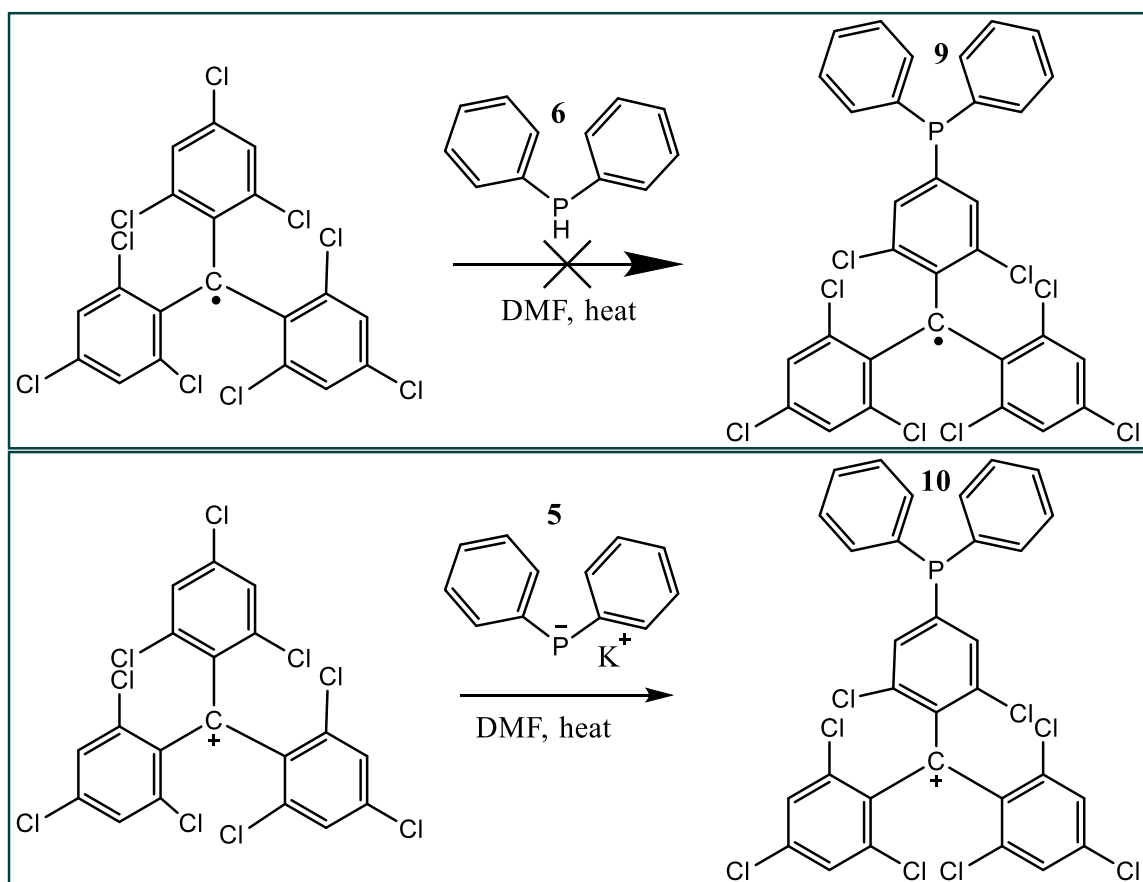
4.1 Introduction

Diphenylphosphines are known compounds, all of which contain a phosphorus atom attached to two phenyl rings. These compounds can sometimes be used as precursors for ligands in catalysis.⁶⁹ Although these compounds are not heteroles, they are close in structure to the dibenzophospholes described in the previous chapter to yield similar compounds with comparable properties.

4.2 Reactions with Diphenylphosphine

Much like the dibenzophosphole, the reactions with TTM radical were unsuccessful. The installation of diphenylphosphine into the TTM radical system resulted in a sticky red substance; however, the ^1H NMR spectrum proved that the TTM radical was reduced back into the HTTM molecule throughout the reaction. The ^{31}P NMR spectrum of this reaction yielded a peak at -40.02ppm, which is consistent with unreacted diphenylphosphine (-40.7ppm)⁷⁰; indicating that the phosphine did not react with the TTM radical. The mishap was also observed when potassium diphenylphosphide (**5**) was reacted with the TTM radical. The ^1H NMR spectrum was indicative of only HTTM and the ^{31}P was denoted evidence of unreacted potassium diphenylphosphide. The TTM⁺ reactions did prove to be fruitful; and it was found that potassium diphenylphosphide could be successfully added to TTM⁺. The ^{31}P NMR of potassium diphenylphosphide reveals a signal for the phosphorus anion at -12.9 ppm, and any variation in the product ^{31}P NMR would indicate a change electron shielding around the phosphorus atom.⁶¹ The ^{31}P NMR chemical shift for the synthesized compound appeared at 41.98 ppm, which is nearly identical to what was observed from the reaction of TTM⁺ and

dibenzophospholide compound (41.40ppm). Given this information, it can be assumed that the diphenylphosphide anion is also attached to one of the TTM rings with chlorine substituents that act as an electron withdrawing group causing the peak to show up more downfield.



Scheme 9. The addition of **6** to the TTM radical and the addition of **5** to the TTM cation

4.3 Experimental

KPh₂-TTM⁺(10) In a nitrogen filled glovebox, 0.1001 (0.113mmol) of potassium diphenylphosphide (**5**) was placed in a 25mL Schlenk flask covered with aluminum foil. 9 mL of anhydrous THF was also added into the flask. 0.0322g (0.143mmol) of **6** was dissolved in 5mL of THF and then subsequently added dropwise into the flask. The initially dark blue color of the solution turned bright red upon addition. The solution was

stirred overnight. The THF was removed *in vacuo* and the resultant product was a sticky red substance with orange fluorescence. ^1H NMR (400 MHz, C_6D_6) δ 7.77 (ddd, $J = 14.2, 8.2, 1.4$ Hz, 3H), 7.55 – 7.47 (m, 3H), 7.02 – 6.88 (m, 10H). ^{31}P NMR (162 MHz, C_6D_6) δ 41.98 (s).

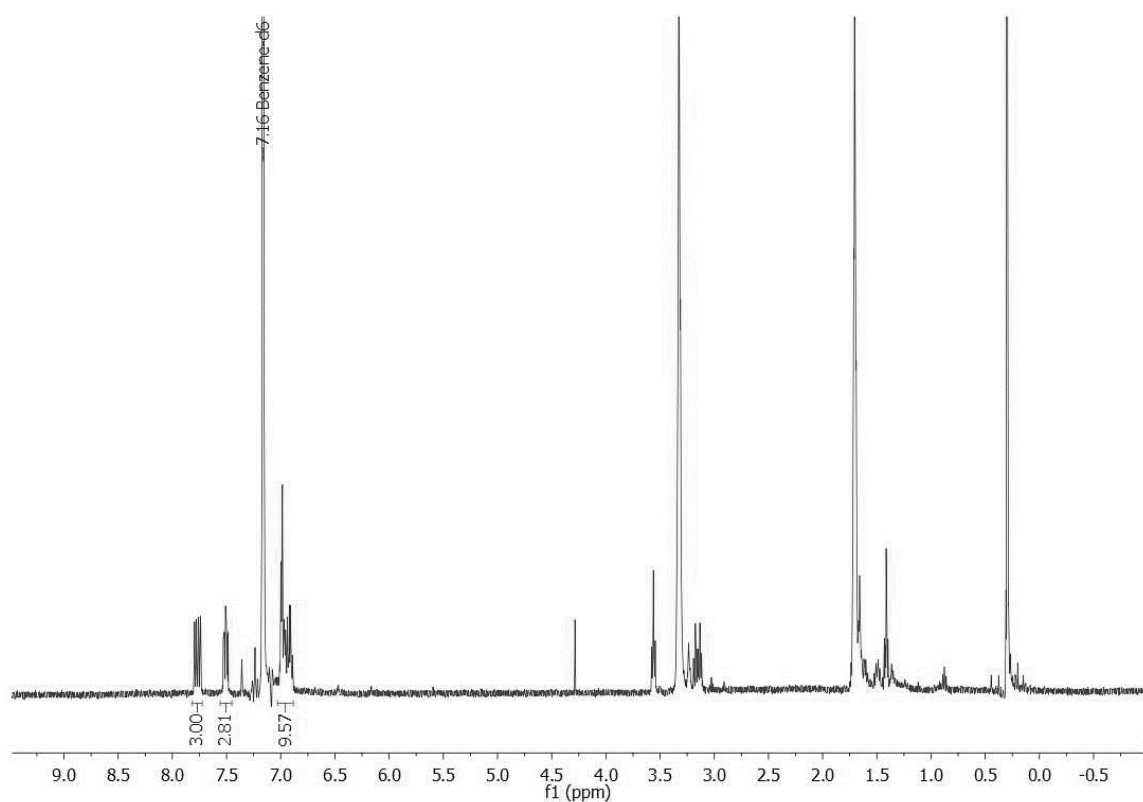


Figure 27. Product **10** ^1H NMR spectrum in C_6D_6 .

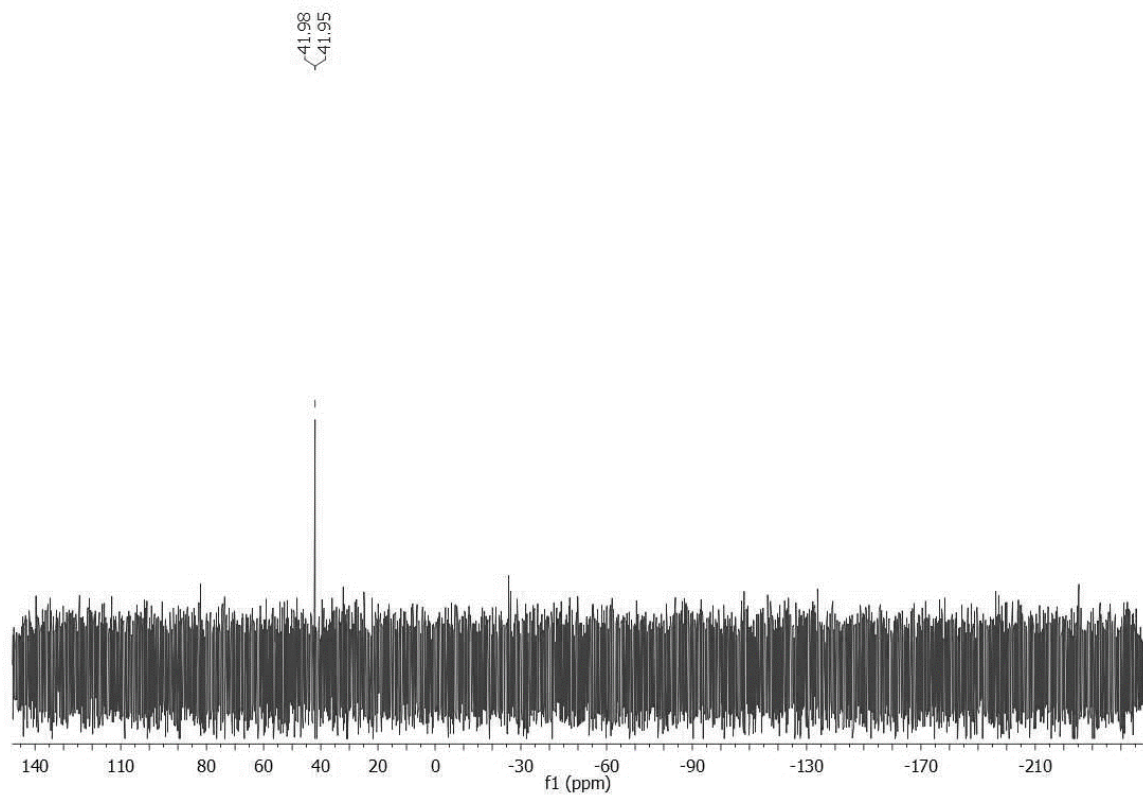


Figure 28. Product **10** ^{31}P NMR spectrum in C_6D_6 .

5. CONCLUSION

Throughout the experimental process of this research, the ultimate goal was to attach a dibenzophosphole moiety to the TTM radical, a molecule with beneficial luminescence due to its open shell system. Four different dibenzophospholes were synthesized, all with the final goal of converting them to the anion so that they could subsequently be added to TTM. Difficulties arose when trying to add the phospholide anion to the TTM radical, however there was success when the TTM^+ was used in place of the radical. The experimental process has proven that the only successful attempts at attaching a dibenzophospholide with TTM involved using an electron-rich phosphorus anion which acts as the Lewis base and the cationic TTM that behaves as the Lewis acid. The two compounds interact in a FLP fashion to form a deep red product with an orange luminescence.

Although there was success, the goal of the research was not fulfilled because the product produced did not contain a radical anywhere throughout the molecule. The cationic TTM is not a paramagnetic molecule, so it falls into the subsection of closed shell systems. This means that the fluorescence emitted from the molecule is caused by transitions between singlet states rather than doublet states. As mentioned before, this fluorescence method is not as efficient as fluorescence from doublet states. Achieving the radical from the cationic TTM can be achieved via a reduction event. This method will be explored during the next phase of experiments.

Exploration of the larger pnictogens will also be attempted. Phosphorus was expected to be a pnictogen that behaved most similarly to nitrogen in the TTM system; however, these assumptions were proven to be inconclusive given the data obtained.

According to the literature, carbazole based units can be incorporated into the TTM radical system with ease; dibenzophosphole based units did not reflect the same chemistry. The difference between the characteristics of the two is most likely attributed to the introduction of a radial node, making the lone pair on the phosphorus atom more diffuse than the lone pair on a nitrogen atom. The increase in nucleophilicity of phosphorus compared to nitrogen proved to only be beneficial in TTM cation reactions. Delving into experiments with larger pnictogens (Ar, Sb, etc) will provide a larger basis for assumptions about how pnictogen heteroles can be used in organoelectronics.

REFERENCES

1. Pelaez, E. A.; Villegas, E. R. In *LED power reduction trade-offs for ambulatory pulse oximetry*, 2007 29th Annual International Conference of the IEEE Engineering in Medicine and Biology Society, 22-26 Aug. 2007; 2007; pp 2296-2299.
2. Ameri, T.; Dennler, G.; Lungenschmied, C.; Brabec, C. J., Organic tandem solar cells: A review. *Energy & Environmental Science* 2009, 2 (4), 347-363.
3. Scharber, M. C.; Mühlbacher, D.; Koppe, M.; Denk, P.; Waldauf, C.; Heeger, A. J.; Brabec, C. J., Design Rules for Donors in Bulk-Heterojunction Solar Cells—Towards 10 % Energy-Conversion Efficiency. 2006, 18 (6), 789-794.
4. Horowitz, G., Organic Field-Effect Transistors. 1998, 10 (5), 365-377.
5. Muccini, M., A bright future for organic field-effect transistors. *Nature Materials* 2006, 5 (8), 605-613.
6. Geffroy, B.; le Roy, P.; Prat, C., Organic light-emitting diode (OLED) technology: materials, devices and display technologies. 2006, 55 (6), 572-582.
7. Fallon, K. J.; Wijeyasinghe, N.; Yaacobi-Gross, N.; Ashraf, R. S.; Freeman, D. M. E.; Palgrave, R. G.; Al-Hashimi, M.; Marks, T. J.; McCulloch, I.; Anthopoulos, T. D.; Bronstein, H., A Nature-Inspired Conjugated Polymer for High Performance Transistors and Solar Cells. *Macromolecules* 2015, 48 (15), 5148-5154.

8. Bronstein, H.; Chen, Z.; Ashraf, R. S.; Zhang, W.; Du, J.; Durrant, J. R.; Shakya Tuladhar, P.; Song, K.; Watkins, S. E.; Geerts, Y.; Wienk, M. M.; Janssen, R. A. J.; Anthopoulos, T.; Sirringhaus, H.; Heeney, M.; McCulloch, I., Thieno[3,2-b]thiophene–Diketopyrrolopyrrole-Containing Polymers for High-Performance Organic Field-Effect Transistors and Organic Photovoltaic Devices. *Journal of the American Chemical Society* 2011, *133* (10), 3272-3275.
9. Sirringhaus, H., 25th Anniversary Article: Organic Field-Effect Transistors: The Path Beyond Amorphous Silicon. 2014, *26* (9), 1319-1335.
10. Zaumseil, J.; Sirringhaus, H., Electron and Ambipolar Transport in Organic Field-Effect Transistors. *Chemical Reviews* 2007, *107* (4), 1296-1323.
11. Yamashita, Y., Organic semiconductors for organic field-effect transistors. *Sci Technol Adv Mater* 2009, *10* (2), 024313-024313.
12. Truong, M. A.; Nakano, K., Syntheses of dibenzo[d,d']benzo[2,1-b:3,4-b']difuran derivatives and their application to organic field-effect transistors. *Beilstein J Org Chem* 2016, *12*, 805-812.
13. Han, T.-H.; Lee, Y.; Choi, M.-R.; Woo, S.-H.; Bae, S.-H.; Hong, B. H.; Ahn, J.-H.; Lee, T.-W., Extremely efficient flexible organic light-emitting diodes with modified graphene anode. *Nature Photonics* 2012, *6*, 105.
14. Dodabalapur, A., Organic light emitting diodes. *Solid State Communications* 1997, *102* (2), 259-267.
15. Explain That Stuff OLEDs (Organic LEDs) and LEPs (light-emitting polymers). <https://www.explainthatstuff.com/how-oleds-and-leps-work.html>.

16. Kaji, H.; Suzuki, H.; Fukushima, T.; Shizu, K.; Suzuki, K.; Kubo, S.; Komino, T.; Oiwa, H.; Suzuki, F.; Wakamiya, A.; Murata, Y.; Adachi, C., Purely organic electroluminescent material realizing 100% conversion from electricity to light. *Nature Communications* 2015, 6, 8476.
17. Pope, M.; Kallmann, H. P.; Magnante, P., Electroluminescence in Organic Crystals. 1963, 38 (8), 2042-2043.
18. Helfrich, W.; Schneider, W. G., Recombination Radiation in Anthracene Crystals. *Physical Review Letters* 1965, 14 (7), 229-231.
19. History of OLEDs. In *OLED Displays and Lighting*, pp 1-11.
20. Tang, C. W.; VanSlyke, S. A., Organic electroluminescent diodes. *Applied Physics Letters* 1987, 51 (12), 913-915.
21. Wakimoto, T.; Murayama, R.; Nagayama, K.; Okuda, Y.; Nakada, H., Organic EL cells with high luminous efficiency. *Applied Surface Science* 1997, 113-114, 698-704.
22. Baldo, M. A.; O'Brien, D. F.; You, Y.; Shoustikov, A.; Sibley, S.; Thompson, M. E.; Forrest, S. R., Highly efficient phosphorescent emission from organic electroluminescent devices. *Nature* 1998, 395 (6698), 151-154.
23. Tremblay, J.-F. The rise of OLED displays.
<https://cen.acs.org/articles/94/i28/rise-OLED-displays.html>.
24. Zhang, S.; Yao, L.; Peng, Q.; Li, W.; Pan, Y.; Xiao, R.; Gao, Y.; Gu, C.; Wang, Z.; Lu, P.; Li, F.; Su, S.; Yang, B.; Ma, Y., Achieving a Significantly Increased Efficiency in Nondoped Pure Blue Fluorescent OLED: A Quasi-Equivalent Hybridized Excited State. 2015, 25 (11), 1755-1762.

25. Uoyama, H.; Goushi, K.; Shizu, K.; Nomura, H.; Adachi, C., Highly efficient organic light-emitting diodes from delayed fluorescence. *Nature* 2012, *492*, 234.
26. Furukawa, T.; Nakanotani, H.; Inoue, M.; Adachi, C., Dual enhancement of electroluminescence efficiency and operational stability by rapid upconversion of triplet excitons in OLEDs. *Scientific Reports* 2015, *5*, 8429.
27. Wagner, M.; Merkt, U.; Chaplik, A. V., Spin-singlet--spin-triplet oscillations in quantum dots. *Physical Review B* 1992, *45* (4), 1951-1954.
28. Shaheen, S. E.; Brabec, C. J.; Sariciftci, N. S.; Padinger, F.; Fromherz, T.; Hummelen, J. C., 2.5% efficient organic plastic solar cells. *Applied Physics Letters* 2001, *78* (6), 841-843.
29. Park, S. H.; Roy, A.; Beaupré, S.; Cho, S.; Coates, N.; Moon, J. S.; Moses, D.; Leclerc, M.; Lee, K.; Heeger, A. J., Bulk heterojunction solar cells with internal quantum efficiency approaching 100%. *Nature Photonics* 2009, *3*, 297.
30. Goushi, K.; Yoshida, K.; Sato, K.; Adachi, C., Organic light-emitting diodes employing efficient reverse intersystem crossing for triplet-to-singlet state conversion. *Nature Photonics* 2012, *6*, 253.
31. Marian, C. M., Spin-orbit coupling and intersystem crossing in molecules. 2012, *2* (2), 187-203.
32. Koziar, J. C.; Cowan, D. O., Photochemical heavy-atom effects. *Accounts of Chemical Research* 1978, *11* (9), 334-341.

33. Liu, Y.; Li, C.; Ren, Z.; Yan, S.; Bryce, M. R., All-organic thermally activated delayed fluorescence materials for organic light-emitting diodes. *Nature Reviews Materials* 2018, 3, 18020.
34. H. Hofeldt, R.; Sahai, R.; Lin, S.-Z., *Heavy Atom Effect on the Phosphorescence of Aromatic Hydrocarbons. II. Quenching of Perdeuterated Naphthalene by Alkali Halide*. 1970; Vol. 53, p 4512-4518.
35. Jankus, V.; Data, P.; Graves, D.; McGuinness, C.; Santos, J.; Bryce, M. R.; Dias, F. B.; Monkman, A. P., Highly Efficient TADF OLEDs: How the Emitter–Host Interaction Controls Both the Excited State Species and Electrical Properties of the Devices to Achieve Near 100% Triplet Harvesting and High Efficiency. 2014, 24 (39), 6178-6186.
36. Komatsu, R.; Sasabe, H.; Inomata, S.; Pu, Y.-J.; Kido, J., High efficiency solution processed OLEDs using a thermally activated delayed fluorescence emitter. *Synthetic Metals* 2015, 202, 165-168.
37. Ai, X.; Evans, E. W.; Dong, S.; Gillett, A. J.; Guo, H.; Chen, Y.; Hele, T. J. H.; Friend, R. H.; Li, F., Efficient radical-based light-emitting diodes with doublet emission. *Nature* 2018, 563 (7732), 536-540.
38. Obolda, A.; Ai, X.; Zhang, M.; Li, F., Up to 100% Formation Ratio of Doublet Exciton in Deep-Red Organic Light-Emitting Diodes Based on Neutral π -Radical. *ACS Applied Materials & Interfaces* 2016, 8 (51), 35472-35478.
39. Peng, Q.; Obolda, A.; Zhang, M.; Li, F., Organic Light-Emitting Diodes Using a Neutral π Radical as Emitter: The Emission from a Doublet. 2015, 54 (24), 7091-7095.

40. Armet, O.; Veciana, J.; Rovira, C.; Riera, J.; Castaner, J.; Molins, E.; Rius, J.; Miravittles, C.; Olivella, S.; Brichfeus, J., Inert carbon free radicals. 8. Polychlorotriphenylmethyl radicals: synthesis, structure, and spin-density distribution. *The Journal of Physical Chemistry* 1987, *91* (22), 5608-5616.
41. Castellanos, S.; Velasco, D.; López-Calahorra, F.; Brillas, E.; Julia, L., Taking Advantage of the Radical Character of Tris(2,4,6-trichlorophenyl)methyl To Synthesize New Paramagnetic Glassy Molecular Materials. *The Journal of Organic Chemistry* 2008, *73* (10), 3759-3767.
42. Kimura, S.; Tanushi, A.; Kusamoto, T.; Kochi, S.; Sato, T.; Nishihara, H., A luminescent organic radical with two pyridyl groups: high photostability and dual stimuli-responsive properties, with theoretical analyses of photophysical processes. *Chemical Science* 2018, *9* (7), 1996-2007.
43. Ai, X.; Chen, Y.; Feng, Y.; Li, F., A Stable Room-Temperature Luminescent Biphenylmethyl Radical. 2018, *57* (11), 2869-2873.
44. Shigehiro, Y.; Kohei, T., A Key Role of Orbital Interaction in the Main Group Element-containing π -Electron Systems. 2005, *34* (1), 2-7.
45. Eisenberger, P.; Kieltsch, I.; Armanino, N.; Togni, A., Mild electrophilic trifluoromethylation of secondary and primary aryl- and alkylphosphines using hypervalent iodine(iii)-CF₃ reagents. *Chemical Communications* 2008, (13), 1575-1577.
46. Wu, B.; Yoshikai, N., Recent developments in synthetic methods for benzo[b]heteroles. *Organic & Biomolecular Chemistry* 2016, *14* (24), 5402-5416.

47. Zassowski, P.; Ledwon, P.; Kurowska, A.; Herman, A. P.; Lapkowski, M.; Cherpak, V.; Hotra, Z.; Turyk, P.; Ivaniuk, K.; Stakhira, P.; Sych, G.; Volyniuk, D.; Grazulevicius, J. V., 1,3,5-Triazine and carbazole derivatives for OLED applications. *Dyes and Pigments* 2018, *149*, 804-811.
48. Lozano-Hernández, L.-A.; Maldonado, J.-L.; Garcias-Morales, C.; Espinosa Roa, A.; Barbosa-García, O.; Rodríguez, M.; Pérez-Gutiérrez, E., Efficient OLEDs Fabricated by Solution Process Based on Carbazole and Thienopyrrolediones Derivatives. *Molecules* 2018, *23* (2), 280.
49. Chan, K. L.; Watkins, S. E.; Mak, C. S. K.; McKiernan, M. J.; Towns, C. R.; Pascu, S. I.; Holmes, A. B., Poly(9,9-dialkyl-3,6-dibenzosilole)—a high energy gap host for phosphorescent light emitting devices. *Chemical Communications* 2005, (46), 5766-5768.
50. Wex, B.; Kaafarani, B. R., Perspective on carbazole-based organic compounds as emitters and hosts in TADF applications. *Journal of Materials Chemistry C* 2017, *5* (34), 8622-8653.
51. Ashe, A. J.; Drone, F. J.; Kausch, C. M.; Kroker, J.; Al-Taweel, S. M., Borepins and group 15 element heteroles. In *Pure and Applied Chemistry*, 1990; Vol. 62, p 513.

52. Frisch, M. J.; Trucks, G. W.; Schlegel, H. B.; Scuseria, G. E.; Robb, M. A.; Cheeseman, J. R.; Scalmani, G.; Barone, V.; Petersson, G. A.; Nakatsuji, H.; Li, X.; Caricato, M.; Marenich, A. V.; Bloino, J.; Janesko, B. G.; Gomperts, R.; Mennucci, B.; Hratchian, H. P.; Ortiz, J. V.; Izmaylov, A. F.; Sonnenberg, J. L.; Williams; Ding, F.; Lipparini, F.; Egidi, F.; Goings, J.; Peng, B.; Petrone, A.; Henderson, T.; Ranasinghe, D.; Zakrzewski, V. G.; Gao, J.; Rega, N.; Zheng, G.; Liang, W.; Hada, M.; Ehara, M.; Toyota, K.; Fukuda, R.; Hasegawa, J.; Ishida, M.; Nakajima, T.; Honda, Y.; Kitao, O.; Nakai, H.; Vreven, T.; Throssell, K.; Montgomery Jr., J. A.; Peralta, J. E.; Ogliaro, F.; Bearpark, M. J.; Heyd, J. J.; Brothers, E. N.; Kudin, K. N.; Staroverov, V. N.; Keith, T. A.; Kobayashi, R.; Normand, J.; Raghavachari, K.; Rendell, A. P.; Burant, J. C.; Iyengar, S. S.; Tomasi, J.; Cossi, M.; Millam, J. M.; Klene, M.; Adamo, C.; Cammi, R.; Ochterski, J. W.; Martin, R. L.; Morokuma, K.; Farkas, O.; Foresman, J. B.; Fox, D. J. *Gaussian 16 Rev. B.01*, Wallingford, CT, 2016.
53. Nyulászi, L.; Hollóczki, O.; Lescop, C.; Hissler, M.; Réau, R., An aromatic–antiaromatic switch in P-heteroles. A small change in delocalisation makes a big reactivity difference. *Organic & Biomolecular Chemistry* 2006, 4 (6), 996-998.
54. Yamaguchi, S.; Fukazawa, A.; Taki, M., Phosphole *P*-Oxide-Containing π -Electron Materials: Synthesis and Applications in Fluorescence Imaging. *Journal of Synthetic Organic Chemistry, Japan* 2017, 75 (11), 1179-1187.
55. Delaere, D.; Dransfeld, A.; Nguyen, M. T.; Vanquickenborne, L. G., Theoretical Study of the Structure–Property Relationship in Phosphole Monomers. *The Journal of Organic Chemistry* 2000, 65 (9), 2631-2636.

56. Katsyuba, S. A.; Burganov, T. I.; Zvereva, E. E.; Zagidullin, A. A.; Miluykov, V. A.; Lönnecke, P.; Hey-Hawkins, E.; Sinyashin, O. G., Conjugation in and Optical Properties of 1-R-1,2-Diphospholes and 1-R-Phospholes. *The Journal of Physical Chemistry A* 2014, *118* (51), 12168-12177.
57. Hibner-Kulicka, P.; Joule, J. A.; Skalik, J.; Bałczewski, P., Recent studies of the synthesis, functionalization, optoelectronic properties and applications of dibenzophospholes. *RSC Advances* 2017, *7* (15), 9194-9236.
58. Hissler, M.; Lescop, C.; Réau, R., π -Conjugated systems: Can phosphole offer more than pyrrole? In *Pure and Applied Chemistry*, 2005; Vol. 77, p 2099.
59. Baumgartner, T.; Réau, R., Organophosphorus π -Conjugated Materials. *Chemical Reviews* 2006, *106* (11), 4681-4727.
60. Yin, J.; Chen, R.-F.; Zhang, S.-L.; Ling, Q.-D.; Huang, W., Theoretical Studies of the Structural, Electronic, and Optical Properties of Phosphafluorenes. *The Journal of Physical Chemistry A* 2010, *114* (10), 3655-3667.
61. Dubinnyi, M. A.; Lesovoy, D. M.; Dubovskii, P. V.; Chupin, V. V.; Arseniev, A. S., Modeling of ^{31}P -NMR spectra of magnetically oriented phospholipid liposomes: A new analytical solution. *Solid State Nuclear Magnetic Resonance* 2006, *29* (4), 305-311.
62. T. Teunissen, H.; B. Hansen, C.; Bickelhaupt, F., A simple one pot synthesis of 1-chlorophospholes. 1996; Vol. Sulfur, p 309-312.

63. Macor, J. A.; Brown, J. L.; Cross, J. N.; Daly, S. R.; Gaunt, A. J.; Girolami, G. S.; Janicke, M. T.; Kozimor, S. A.; Neu, M. P.; Olson, A. C.; Reilly, S. D.; Scott, B. L., Coordination chemistry of 2,2'-biphenylenedithiophosphate and diphenyldithiophosphate with U, Np, and Pu. *Dalton Transactions* 2015, 44 (43), 18923-18936.
64. Oukhrib, A.; Bonnafoux, L.; Panossian, A.; Waifang, S.; Nguyen, D. H.; Urrutigoity, M.; Colobert, F.; Gouygou, M.; Leroux, F. R., Novel C1-symmetric dibenzophosphole ligands: application in hydroformylation reactions. *Tetrahedron* 2014, 70 (7), 1431-1436.
65. Ashby, E. C.; Gurumurthy, R.; Ridlehuber, R. W., Investigation of the purity of alkali metal diphenylphosphides and their reactions with organic halides. Evidence for single electron transfer. *The Journal of Organic Chemistry* 1993, 58 (21), 5832-5837.
66. Carilla, J.; Fajarí, L.; Juliá, L.; Riera, J.; Viadel, L., Two functionalized free radicals of the tris(2,4,6-trichlorophenyl)methyl radical series. Synthesis, stability and EPR analysis. *Tetrahedron Letters* 1994, 35 (35), 6529-6532.
67. Stephan, D. W., "Frustrated Lewis pairs": a concept for new reactivity and catalysis. *Organic & Biomolecular Chemistry* 2008, 6 (9), 1535-1539.
68. Stephan, D. W., Frustrated Lewis Pairs. *Journal of the American Chemical Society* 2015, 137 (32), 10018-10032.
69. Reznikov, A. N.; Skvortsov, N. K., [2-(6,6-Dimethylbicyclo[3.3.1]hept-2-enyl)ethyl]-diphenylphosphine and phosphine oxide. Coordination properties and application in catalysis. *Russian Journal of General Chemistry* 2011, 78 (2), 197.
70. Diphenylphosphine. In *Encyclopedia of Reagents for Organic Synthesis*.